

MULTIFREQUENCY OBSERVATIONS OF BLAZARS. III. THE SPECTRAL SHAPE OF THE RADIO TO X-RAY CONTINUUM

L. M. J. BROWN, E. I. ROBSON, W. K. GEAR, AND D. H. HUGHES

School of Physics and Astronomy, Lancashire Polytechnic

M. J. GRIFFIN

Department of Physics, Queen Mary College

B. J. GELDZAHLER

Applied Research Corporation

P. R. SCHWARTZ

E. O. Hubert Center for Space Research, US Naval Research Laboratory

M. G. SMITH

United Kingdom Infrared Telescope

A. G. SMITH, D. W. SHEPHERD, AND J. R. WEBB

Rosemary Hill Observatory, University of Florida

E. VALTAOJA

Turku University Observatory, University of Turku

AND

H. TERASRANTA AND E. SALONEN

Radio Laboratory, Helsinki University of Technology

Received 1987 October 26; accepted 1988 October 3

ABSTRACT

We present multifrequency, quasi-simultaneous spectra for a sample of 11 blazars. The spectral shape of the violently variable millimeter to ultraviolet flux is consistent with emission from a very compact *single* component which becomes self-absorbed at wavelengths longer than ~ 3 mm. The centimeter emission can be attributed to a separate, more slowly varying component. Three out of four optically violent variable (OVV) quasars also exhibit evidence of a "UV excess" component. Throughout the millimeter-UV region, the *flattest* spectral slopes, observed when the sources are bright, are all close to -0.7 . However, the *steepest* slopes (observed when the sources are fainter) become *steeper* as one progresses to *shorter wavelength*. We interpret this in terms of successive injections or reaccelerations of electrons in a flaring component, superposed on the more slowly varying component which peaks at centimeter wavelengths. We deduce values for the size of the flaring regions of 10^{-3} – 10^{-1} pc and magnetic fields of order 1 G. We also deduce that photon energy densities may dominate over magnetic field energy densities, in which case inverse Compton scattering may be the dominant energy loss mechanism in the flaring components.

Subject headings: BL Lacertae objects — quasars — radiation mechanisms — radio sources: variable

I. INTRODUCTION

The highly polarized, violently variable millimeter to ultraviolet emission from blazars originates in a compact ($\lesssim 1$ mas) core (Gear *et al.* 1986; Simon *et al.* 1985). The study of the millimeter to ultraviolet continuum spectral shape and variability of blazars can thus elucidate the emission mechanisms operating in these very compact regions. At centimeter and longer wavelengths, however, there is generally a contribution to the emission from extended (1–10 mas) components. Spectral decompositions of the radio spectra of blazars by means of VLBI observations are thus highly important in order to isolate the emission from the compact core. To date such spectral decompositions have been performed on only a small number of blazars, e.g., 3C 345 (Unwin *et al.* 1983).

The emission from blazars exhibits variability at all observed wavelengths, on time scales ranging from roughly months at centimeter and longer wavelengths, through roughly weeks at submillimeter wavelengths, to roughly days or less in the ultraviolet. Because of the relative scarcity of X-ray data obtained to date on blazars, the variability time scale at X-ray

wavelengths is not well determined but observations point to different time scales in different sources, ranging from roughly months (0735+178; Bregman *et al.* 1984) to roughly days (3C 446; Brown *et al.* 1986). Recent work by Lawrence *et al.* (1987) and McHardy and Czerny (1987) indicates that, in at least some active galaxies, there are no preferred X-ray variability time scales and that the differences in measured time scales may in fact be due simply to the varying observational sampling rates. Thus, simple measures of X-ray variability time scales need to be treated with caution. We investigate the variability of blazars in detail in a companion paper (Brown 1989; henceforth Paper IV).

In order to determine the continuum spectral shape of a source, it is necessary to obtain quasi-simultaneous observations over as wide a spectral range as possible. To this end, we have been monitoring since 1982 a sample of 13 blazars in 11 wave bands between 1 and 1100 μm . The results of this monitoring program up to early 1984 have been discussed in Gear *et al.* (1985, 1986; henceforth Papers I and II, respectively). Subsequent results are included in this paper. Wherever possible,

we have combined our near-infrared to submillimeter data with observations obtained at centimeter, millimeter, and optical wavelengths and with centimeter to X-ray data taken from data archives and the literature.

In this paper we present quasi-simultaneous centimeter to optical spectra for 11 of the 13 sources discussed in Papers I and II. Where possible the spectra also include ultraviolet and X-ray data. In each case the quasi-simultaneous spectrum which is presented and discussed represents the most complete spectral coverage we possess on the source concerned.

II. OBSERVATIONS

The criteria for the selection of our sample of sources were given in Paper I. Of this sample, 1413 + 135 is not discussed here because to date we have obtained very little data on this source. The blazar 2251 + 158 has also been excluded because it is only $\sim 10''$ away from a star, the emission from which we suspect may have contaminated some of the near-infrared observations. The 11 sources which we shall be discussing are listed in Table 1. These sources by no means constitute a full sample. However, as Table 1 demonstrates, both BL and Lac objects and OVV quasars are well represented, and the sources cover a wide range in redshift and luminosity. Thus they should be representative of the class of blazars as a whole.

The reduction of our millimeter to infrared data was described in Paper I, while the reduction procedures for the centimeter and optical observations were given in Brown *et al.* (1986). Observations at 2.6 and 1.35 cm and 8.1 and 3.4 mm were obtained at the Metsahovi Radio Research Station, Finland; the reduction procedures are described in Salonen *et al.* (1988).

IRAS observations were obtained from the *IRAS* "Pointed Observations" hard copy data archive at the Rutherford Appleton Laboratory, UK. The quoted flux densities have been converted from the *IRAS* band fluxes using the 1985 November absolute calibration (Young *et al.* 1985). Only observations obtained using the DPS macros are included here. The absolute calibration of the DPS observations has a quoted uncertainty of 2%, 5%, 5%, and 10% at 12, 25, 60, and 100 μm , respectively. The uncertainties quoted here are the sum of the statistical uncertainties and assumed photometric uncertainties of 10% added in quadrature plus the absolute calibration uncertainties.

We have supplemented our data with additional data obtained from the literature. Centimeter data were taken for all the sources in our sample from Aller *et al.* (1985). Millimeter

TABLE 1
SAMPLE

Source	Classification ^a	Redshift
0235 + 164	B	0.852
0420 - 014	B	0.915
0735 + 178	B	0.424
0736 + 017	O	0.191
0851 + 202 (OJ 287)	B	0.306
1253 - 055 (3C 79)	O, S	0.538
1308 + 326	B	0.996
1641 + 399 (3C 345)	O, S	0.595
1921 - 293 (OV 236)	B	0.352
2200 + 420 (BL Lac)	B, S	0.07
2223 - 052 (3C 446)	O	1.404

^a B: BL Lac object; O: OVV Quasar; S: Superluminal source.

TABLE 2
ADOPTED VALUES OF $E(B-V)$

Source	$E(B-V)$
0235 + 164	0.03
0420 - 014	0.07
0735 + 178	0.07
0736 + 017	0.12
0851 + 202	0.02
1253 - 055	0.01
1308 + 326	0.01
1641 + 399	0.00
1921 - 293	0.12
2200 + 420	0.36
2223 - 052	0.05

data were from Salonen *et al.* (1988). *IRAS* data were taken for 0736 + 017 from Landau *et al.* (1986) and for 3C 345 from Bregman *et al.* (1986). Optical data were taken from Holmes *et al.* (1984), Moles *et al.* (1985), Bregman *et al.* (1984, 1986), Mufson *et al.* (1985), Doroshenko *et al.* (1986), and Landau *et al.* (1986). Ultraviolet data were taken from Worrall *et al.* (1982), Bregman *et al.* (1984, 1986), Hanson and Coe (1985), Malkan and Moore (1986), and Landau *et al.* (1986). X-ray data were taken for OJ 287 from Pollock *et al.* (1985) and for 3C 446 from Brown *et al.* (1986). X-ray data on 3C 279 were generously given by A. Cavaliere and L. Piro.

Where necessary, the near-infrared through ultraviolet data were corrected for galactic extinction by adopting values for $E(B-V)$ predicted by the method of Burstein and Heiles (1982) and applying the reddening law of Seaton (1979). No dereddening has been performed on the near-infrared fluxes of those sources for which the effect at these wavelengths is less than 3%, i.e., within the observational uncertainties. The values adopted for $E(B-V)$ are shown in Table 2. Of the 11 sources listed in Table 1, only one, BL Lac, shows evidence for significant emission from a host galaxy. It is therefore necessary to correct our near-infrared and optical data on BL Lac for the (aperture-dependent) contribution from the host galaxy. The correction procedure is described in detail in Brown (1988). The flux densities calculated for the host galaxy at $U(0.36 \mu\text{m})$, $B(0.44 \mu\text{m})$, $V(0.55 \mu\text{m})$, $J(1.25 \mu\text{m})$, $H(1.65 \mu\text{m})$, $K(2.2 \mu\text{m})$, and $L(3.45 \mu\text{m})$ in various apertures between $6''$ and $12''$ are presented in Table 3. The uncertainties are difficult to estimate, but are of the order of 30% which is assumed here for all wavelengths and is added to the observational uncertainty to give the total uncertainty of the flux density of BL Lac at the wavelength concerned.

Our observational results are presented in Tables 4-9. These observations represent an extensive data base which was

TABLE 3
DERIVED FLUX DENSITIES (mJy) FOR THE HOST GALAXY OF BL LAC

COLOR	APERTURE			
	6"	8"	10"	12"
<i>U</i>	0.14	0.18	0.21	0.23
<i>B</i>	0.50	0.66	0.76	0.82
<i>V</i>	1.2	1.6	1.8	1.9
<i>J</i>	5.2	6.8	7.8	8.4
<i>H</i>	5.7	7.5	8.6	9.4
<i>K</i>	3.6	4.7	5.4	5.9
<i>L</i>	2.0	2.7	3.1	3.3

TABLE 4
SUBMILLIMETER-INFRARED FLUX DENSITIES

SOURCE	UT DATE	WAVELENGTH (μm)								
		1.25 (mJy)	1.65 (mJy)	2.20 (mJy)	3.45 (mJy)	10 (mJy)	20 (mJy)	370 (Jy)	770 (Jy)	1070 (Jy)
0235 + 164	1984 Aug 1-3	< 225
	1984 Nov 28	1.0(0.1)	1.9(0.1)	3.0(0.1)	4.8(0.7)
0420-014	1986 Feb 24	3.5(0.8)
0735 + 178	1984 Apr 18-21	6.6(0.3)	9.8(0.4)	13.9(0.5)	24.8(1.4)	43(10)
	1984 Nov 28	2.9(0.1)	4.6(0.4)	6.9(0.3)	13.8(2.0)
	1986 Jan 16	< 0.6
	1986 Feb 19	7.1(0.4)	9.8(0.5)	13.7(0.7)	24.0(2.0)
0736 + 017	1984 Apr 18-21	3.5(0.1)	5.1(0.2)	8.0(0.2)	12.5(1.0)
	1984 Nov 28	4.9(0.2)	8.3(0.8)	13.1(0.4)	26.6(1.5)
	1986 Jan 16	< 1.2	1.1(0.3)
	1986 Feb 19	2.9(0.1)	4.1(0.2)	6.6(0.3)	11.2(1.3)
0851 + 202	1984 Mar 8	26.7(1.3)	35.9(1.8)	47.5(2.4)	82.3(4.1)
	1984 Apr 18-21	6.5(0.1)	9.5(0.2)	12.8(0.2)	24.8(1.5)	48(12)	4.6(0.3)
	1984 Nov 28	3.0(0.1)	4.6(0.2)	7.1(0.2)	14.6(1.3)	4.3(1.0)
	1984 Dec 22	4.0(0.2)	5.9(0.3)	9.6(0.5)	17.2(0.9)
	1985 Jan 5-8	4.6(1.4)	4.9(1.0)	5.9(0.9)
	1985 Feb 22	10.6(0.5)	13.9(0.7)	20.0(1.0)	32.4(1.6)
	1985 Mar 5	7.1(1.0)	7.0(1.1)
	1985 Apr 24	16.5(0.8)	22.4(1.1)	29.8(1.5)
	1986 Jan 16	1.5(0.4)	1.3(0.4)
	1986 Feb 19-24	5.1(0.2)	7.8(0.2)	11.8(0.3)	23.7(0.3)	70(15)	3.9(0.5)	2.9(0.3)
1253-055	1984 Apr 18-21	1.7(0.1)	2.9(0.1)	4.1(0.2)	8.6(0.9)	< 75	4.1(0.5)
	1984 Nov 28	2.7(0.1)	4.1(0.4)	7.0(0.4)
	1985 Feb 22	2.3(0.1)	3.4(0.2)	6.0(0.3)	13.4(0.7)
	1985 Apr 24	1.0(0.1)	2.3(0.1)	3.6(0.2)
	1985 Jun 12	1.8(0.1)	2.9(0.1)	4.8(0.2)	11.6(0.6)
	1985 Jun 14	2.2(0.1)	3.6(0.2)	5.8(0.3)	14.4(0.7)
	1986 Feb 19-24	2.0(0.2)	3.0(0.1)	4.6(0.5)	7.6(0.8)	3.0(0.7)	3.1(0.4)
1308 + 326	1984 Apr 18-21	2.3(0.2)	3.6(0.2)	5.1(0.2)	12.2(1.3)	< 40	1.8(0.4)
	1984 Aug 1-3	< 5.8	...
	1985 Feb 22	5.6(0.3)	7.8(0.4)	11.8(0.6)	21.2(1.1)
	1985 Jun 12	2.3(0.1)	3.4(0.2)	5.3(0.3)	10.2(0.5)
	1986 Feb 21-24	0.5(0.1)	0.6(0.1)	0.8(0.1)	1.0(0.2)
1641 + 399	1984 Mar 8	2.5(0.1)	3.8(0.2)	5.6(0.3)	12.6(0.6)
	1984 Apr 18-21	2.9(0.2)	4.3(0.3)	6.6(0.4)	15.1(1.7)	46(9)	4.8(0.9)	5.0(0.5)
	1984 May 19	3.2(0.2)	4.9(0.2)	7.0(0.3)	15.4(0.8)
	1984 Aug 1-3	5.6(0.1)	8.1(0.4)	12.2(0.39)	24.0(1.6)	95(18)	< 260	...	5.0(0.9)	6.0(0.9)
	1985 Mar 5	3.2(0.5)	3.5(0.4)
	1985 Apr 24	2.1(0.1)	3.1(0.2)	5.1(0.3)	10.5(0.5)
	1985 Jun 21	2.2(0.1)	3.2(0.2)	5.1(0.3)	8.8(0.4)
	1986 Jan 10-12	2.4(0.4)	3.6(0.4)
1986 Feb 20-24	3.0(0.2)	4.6(0.2)	7.3(0.4)	3.4(0.7)	3.4(0.3)	
1921-293	1983 Sep 18	3.5(0.6)	3.8(0.4)
	1984 Apr 18-21	6.1(1.7)	3.8(0.3)
	1984 Aug 1-3	5.1(0.1)	8.3(0.4)	12.9(0.3)	23.0(2.1)	70(14)	160(35)	6.5(1.8)	9.0(1.9)	6.0(0.7)
	1986 Feb 23	< 2.1
2200 + 420	1984 Apr 19	2.3(0.5)
	1984 Aug 1-3	14.6(0.1)	20.9(0.8)	27.4(0.7)	41.4(1.9)	90(14)	240(64)	...	< 2.5	2.5(0.8)
	1985 Aug 24-25	21.4(1.1)	29.9(1.5)	40.5(2.0)	64.6(3.2)
	1986 Feb 20-24	< 3.0	1.3(0.3)
2223-052	1984 Jul 18	1.43(0.04)	...	3.6(0.1)	9.7(0.3)
	1984 Aug 1-6	1.27(0.02)	2.1(0.1)	3.2(0.1)	7.5(0.7)	37(10)	< 8	5.2(1.1)
	1984 Oct 14	1.30(0.03)	2.5(0.1)	3.7(0.1)	11.2(3.3)
	1984 Dec 22	0.8(0.1)	1.3(0.1)	2.0(0.1)	3.8(0.2)
	1985 Jun 13	0.62(0.03)	1.1(0.1)	1.7(0.1)
	1985 Jun 20	1.30(0.04)	1.6(0.1)	2.1(0.1)
	1985 Aug 24-25	0.4(0.1)	...	0.9(0.1)

NOTE.—The observational uncertainties are enclosed in parentheses.

TABLE 5
NRAO MILLIMETER FLUX DENSITIES (Jy)

SOURCE	DATE	WAVELENGTH (mm)		
		1.3	2.0	3.3
0235+164.....	1984 Mar 3-6	...	<1.3	1.8(0.2)
0420-014.....	1986 Mar 3-6	...	3.7(0.5)	5.0(0.4)
0735+178.....	1986 Mar 3-6	...	<1.0	1.3(0.2)
0736+017.....	1986 Mar 3-6	...	<1.1	1.7(0.1)
0851+202.....	1984 Feb 29-Mar 6	...	5.8(1.0)	...
	1986 Mar 3-6	5.1(0.6)	7.7(0.8)	7.4(0.4)
1253-055.....	1984 Feb 29-Mar 6	...	3.0(0.4)	...
	1986 Mar 3-6	4.6(0.9)	6.1(0.7)	7.6(0.5)
1308+326.....	1986 Mar 3-6	1.1(0.3)	1.6(0.3)	1.4(0.1)
1641+399.....	1984 Feb 29-Mar 6	...	6.3(0.8)	...
	1986 Mar 3-6	3.0(0.7)	4.5(0.5)	7.5(0.5)
1921-293.....	1986 Mar 3-6	4.2(0.8)	5.4(0.6)	6.3(0.4)
2200+420.....	1986 Mar 3-6	2.1(0.4)	2.0(0.4)	2.0(0.1)

TABLE 6
IRAS FLUX DENSITIES (mJy)

SOURCE	DATE	WAVELENGTH (μ m)			
		12	25	60	100
0235+164.....	1983 Jul 31	64(18)	...	244(45)	500(150)
0420-014.....	1984 Aug 26-31	114(30)	...	286(37)	...
0735+178.....	1983 Oct 6-13	79(22)	147(43)	279(42)	...
	1983 Nov 14	90(25)	197(52)	320(66)	...
0851+202.....	1983 Apr 15-May 30	170(16)	406(48)	790(75)	1475(225)
	1983 Oct 24-Nov 16	252(18)	444(46)	1082(100)	1785(260)
1641+399.....	1983 Jul 17-Sep 9	123(10)	290(25)	730(60)	1390(200)
2200+420.....	1983 May 30-Jul 16	120(11)	225(20)	455(40)	...
2223-052.....	1983 Nov 8-11	172(17)	340(40)	915(90)	1935(300)

obtainable only through the cooperation of a number of observing groups. We have chosen to present our results uncorrected for galactic extinction or emission from a host galaxy, or both, for consistency with the results published in Papers I and II and elsewhere in the literature. However, we have used the corrected data for plotting the blazar spectra, for deriving spectral slopes and as the basis for all conclusions drawn in this paper.

III. RESULTS

Figure 1*a-k* shows one quasi-simultaneous spectrum for each of the sources from our sample. We have combined into one "quasi-simultaneous" spectrum all available radio to near-infrared data obtained less than ~ 1 month apart and have added optical to X-ray observations if they were obtained within less than 9 days of the near-infrared data. This is inevitably a compromise: ideally one would wish to produce spectra for which the radio through X-ray observations were obtained at most a few days apart. However, such a program is not at present a practical proposition for a large sample of sources, because of limitations on telescope time and the difficulty of coordinating multifrequency observations involving many different wavelength regimes.

IV. DISCUSSION

a) Overall Spectral Properties

The spectra presented in Figure 1 are representative of the results obtained from combining quasi-simultaneous centimeter through X-ray data on our sample of sources. They

illustrate the following important characteristics of the spectra of blazars.

1. The millimeter to UV blazar spectra shown in this paper are smoothly continuous, and in Paper IV we show that the millimeter to optical variability is well correlated. We therefore believe that the millimeter to optical emission is dominated by a single violently variable component.

2. There are two schools of thought concerning the description of the overall radio through UV/X-ray continuum energy distribution of blazars: that the spectra can be best described by a combination of power laws, or, alternatively by a singly varying function such as a parabola. Brown (1988) discusses this in detail and conclude that the available observational data are insufficient to discriminate between the two representations apart from some particular examples. But, by Occam's razor, we select power laws, which may be understood readily in terms of emission from a power-law energy distribution of electrons, while acknowledging that at high frequencies curvature may be present due to electron energy losses and that synchrotron self-absorption will be present at low frequencies (see characteristics 3-5).

3. Spectral steepening generally occurs in the mid/near-infrared. Such steepening is usually characterized by a clear spectral break occurring over less than two octaves in frequency (see, e.g., Fig. 1*e*, 1*h*, and 1*i*).

4. In the near-infrared, the spectra of the majority of the blazars are well fitted by power laws, with further spectral steepening occurring in the optical/ultraviolet. Some sources exhibit a high-frequency cutoff, characterized by a spectral slope of less than -3 and rapid negative curvature of the

TABLE 7
VLA CENTIMETER FLUX DENSITIES (Jy)

SOURCE	DATE	WAVELENGTH (cm)			
		1.3	2	6	20
0235 + 164.....	1984 Jul 25	1.184(0.015)	1.304(0.005)	1.699(0.010)	1.929(0.016)
	1984 Nov 16-17	0.840(0.054)	0.824(0.024)	1.030(0.007)	1.511(0.003)
	1985 Oct 26	2.359(0.069)	2.266(0.033)	1.138(0.010)	0.819(0.002)
	1985 Oct 28	1.669(0.033)	1.799(0.015)	1.154(0.004)	0.844(0.002)
	1985 Dec 3	1.180(0.018)	1.496(0.009)	1.146(0.003)	0.824(0.002)
	1986 Feb 24	...	1.700(0.002)	1.411(0.005)	0.872(0.024)
0420 - 014.....	1984 Jul 25	3.329(0.080)	4.180(0.078)	3.009(0.076)	1.973(0.053)
	1984 Nov 16-17	5.620(0.183)	5.172(0.080)	3.375(0.018)	2.153(0.008)
	1985 Oct 26-28	6.78(0.10)	7.82(0.20)	4.20(0.01)	2.23(0.01)
	1985 Dec 3	8.789(0.179)	9.592(0.114)	4.200(0.008)	...
	1986 Feb 24	...	7.02(0.01)	4.794(0.019)	2.354(0.044)
0735 + 178.....	1984 Apr 18	...	2.060(0.022)	1.933(0.003)	1.869(0.004)
	1984 Nov 16-17	1.19(0.231)	1.481(0.116)	1.792(0.013)	1.915(0.013)
	1985 Oct 28	1.857(0.028)	1.999(0.015)	1.606(0.005)	1.697(0.014)
	1985 Dec 3	1.337(0.012)	2.076(0.008)	1.616(0.004)	1.827(0.004)
	1986 Feb 24	...	1.56(0.02)	1.665(0.006)	1.731(0.032)
0736 + 017.....	1984 Apr 18	...	1.948(0.022)	1.907(0.004)	2.135(0.005)
	1984 Nov 16-17	1.898(0.340)	1.784(0.108)	1.683(0.012)	1.923(0.008)
	1985 Oct 28	2.237(0.041)	2.226(0.022)	2.355(0.008)	2.065(0.004)
	1985 Dec 3	2.178(0.019)	2.238(0.011)	2.119(0.005)	2.002(0.005)
	1986 Feb 24	...	2.73(0.03)	2.295(0.017)	2.007(0.029)
0851 + 202.....	1984 Apr 18	...	7.295(0.062)	3.940(0.006)	2.508(0.005)
	1984 Nov 16-17	3.970(1.103)	4.907(0.461)	2.592(0.018)	1.780(0.012)
	1985 Oct 28	5.656(0.040)	4.977(0.049)	3.951(0.012)	2.366(0.013)
	1985 Dec 3	6.638(0.105)	5.725(0.036)	3.562(0.009)	2.309(0.004)
	1986 Feb 24	...	4.54(0.06)	3.078(0.017)	2.451(0.029)
1253 - 055.....	1984 Apr 18	...	9.859(0.102)	10.347(0.042)	10.111(0.098)
1308 + 326.....	1984 Apr 18	...	3.194(0.017)	2.011(0.002)	1.472(0.016)
	1984 Jul 29	2.782(0.084)	2.747(0.049)	2.101(0.005)	1.484(0.009)
	1984 Nov 16-17	4.142(0.116)	3.807(0.035)	2.180(0.005)	1.463(0.013)
	1985 Dec 3	2.756(0.010)	3.006(0.008)	2.467(0.007)	1.57(0.21)
1641 + 399.....	1984 Apr 18	...	12.723(0.003)	12.252(0.022)	8.587(0.030)
	1984 Jul 25	11.061(0.373)	12.034(0.163)	12.403(0.067)	8.918(0.042)
1921 - 293.....	1984 Apr 13	...	9.738(0.056)	7.996(0.016)	6.842(0.051)
	1984 Jul 25	9.341(0.158)	12.464(0.078)	8.246(0.044)	...
	1984 Nov 16-17	14.206(0.942)	14.518(0.150)	9.120(0.020)	6.449(0.037)
	1985 Oct 26	10.351(0.351)	14.721(0.286)	9.501(0.099)	7.190(0.033)
	1985 Dec 3	10.351(0.351)	14.721(0.286)	9.501(0.099)	7.190(0.033)
	1986 Feb 26	9.760(0.368)	11.728(0.218)	11.796(0.602)	9.329(0.259)
2200 + 420.....	1984 Apr 13	...	2.342(0.013)	3.012(0.006)	...
	1984 Jul 25	2.402(0.053)	2.789(0.027)	2.674(0.014)	2.580(0.012)
	1984 Nov 16-17	2.440(0.102)	2.381(0.051)	2.833(0.024)	2.566(0.017)
	1985 Oct 26	2.183(0.042)	2.541(0.018)	2.113(0.003)	2.440(0.005)
	1985 Dec 3	1.305(0.035)	2.264(0.015)	1.954(0.002)	2.382(0.005)
	1986 Feb 26	1.790(0.071)	1.857(0.028)	1.910(0.086)	1.702(0.013)
2223 - 052.....	1984 Apr 13	...	8.147(0.057)	5.905(0.011)	5.843(0.010)
	1984 Jul 25	9.232(0.103)	9.118(0.076)	5.966(0.028)	5.971(0.024)
	1985 Oct 26	5.478(0.156)	5.789(0.086)	4.921(0.012)	6.087(0.017)
	1985 Dec 3	3.961(0.079)	4.987(0.054)	4.679(0.010)	6.135(0.024)
	1986 Feb 26	4.107(0.128)	4.069(0.043)	4.028(0.057)	6.626(0.054)

spectrum. Such cutoffs usually occur at ultraviolet or shorter wavelengths (see, e.g., 3C 446: Fig. 1*k*) but may on occasion be seen in the near-infrared to optical (e.g., 0235 + 164; Fig. 1*a*).

5. A spectral turnover or flattening occurs at millimeter-submillimeter wavelengths, with the spectral slope at frequencies below the turnover ranging from ~ 0 to ~ 1.5 .

6. The 1-6 cm emission in general exhibits two important properties: (a) an excess over the extrapolation of the flattish millimeter/submillimeter spectrum and (b) a spectral turnover at $\sim 2-5$ cm (see Fig. 2). These properties suggest strongly that

the emission in this spectral region is dominated by a synchrotron emission component (separate from the violently variable flaring components dominating at higher frequencies) which becomes optically thick at $\sim 2-5$ cm. The emission from this component would be expected to underlie the flaring emission components and may be identified with a "quiescent" emission component on which the flaring components are superposed (cf. the behavior of the quasar 3C 273; Clegg *et al.* 1983; Robson *et al.* 1983). Some variability is in fact seen at centimeter wavelengths, but this may largely be due to variations in

TABLE 8
B BAND FLUX DENSITIES (mJy)

Source	Date (U.T.)	B	Source	Date (U.T.)	B
0235+164.....	1982 Feb 15	0.6 ± 0.1	0851+202.....	1985 Dec 15	1.3 ± 0.1
	1982 Feb 21	0.5 ± 0.1		1986 Jan 6	1.4 ± 0.1
	1982 Oct 12	0.15 ± 0.03		1986 Feb 2	1.2 ± 0.1
	1982 Oct 22	0.09 ± 0.02		1986 Mar 7	1.1 ± 0.1
	1982 Dec 19	0.30 ± 0.03		1984 Nov 24	0.80 ± 0.04
	1982 Dec 22	0.38 ± 0.04		1984 Nov 29	0.37 ± 0.06
	1983 Sep 6	0.20 ± 0.02		1985 Jan 15	1.3 ± 0.1
	1983 Oct 4	0.40 ± 0.03		1985 Jan 21	3.1 ± 0.1
	1984 Jan 3	0.16 ± 0.02		1985 Jan 26	2.5 ± 0.3
	1984 Sep 27	0.08 ± 0.01		1985 Feb 16	2.6 ± 0.4
	1984 Oct 26	0.13 ± 0.01		1985 Feb 19	1.9 ± 0.4
	1984 Nov 16	0.06 ± 0.01		1985 Mar 15	2.8 ± 0.3
	1985 Oct 16	0.08 ± 0.01		1985 Mar 19	1.6 ± 0.2
	1985 Nov 13	0.09 ± 0.01		1985 Mar 23	1.7 ± 0.4
	1986 Jan 12	0.08 ± 0.02		1985 Apr 10	2.0 ± 0.1
1986 Jan 31	0.08 ± 0.01	1985 Nov 17	1.1 ± 0.1		
0420-014.....	1984 Oct 23	0.24 ± 0.07	1985 Nov 19	0.89 ± 0.04	
	1984 Nov 23	0.23 ± 0.05	1985 Dec 11	3.8 ± 0.3	
	1984 Nov 27	0.14 ± 0.03	1985 Dec 15	0.9 ± 0.1	
	1984 Dec 29	< 0.6 ^a	1985 Dec 17	1.2 ± 0.3	
	1985 Jan 22	0.20 ± 0.04	1986 Jan 6	0.8 ± 0.1	
	1985 Oct 15	0.41 ± 0.08	1986 Jan 12	0.77 ± 0.05	
	1985 Nov 9	0.29 ± 0.05	1986 Jan 14	0.76 ± 0.08	
	1985 Nov 16	0.27 ± 0.04	1986 Jan 31	0.42 ± 0.08	
	1986 Jan 6	0.45 ± 0.05	1986 Feb 1	0.9 ± 0.2	
	1986 Jan 31	0.22 ± 0.02	1986 Feb 13	0.95 ± 0.14	
	0735+178.....	1982 Mar 17	3.0 ± 0.4	1986 Mar 6	1.5 ± 0.1
1982 Mar 18		3.4 ± 0.2	1986 Mar 31	1.8 ± 0.2	
1982 Nov 24		3.0 ± 0.5	1253-055.....	1982 Mar 3	0.5 ± 0.1
1982 Dec 18		4.0 ± 0.6	1982 Mar 18	0.56 ± 0.02	
1983 Mar 3		2.0 ± 0.3	1982 Mar 31	0.6 ± 0.1	
1983 Nov 2		2.4 ± 0.4	1982 May 16	1.0 ± 0.3	
1983 Nov 12		2.0 ± 0.1	1983 Mar 10	1.1 ± 0.1	
1984 Jan 8		1.4 ± 0.1	1983 May 12	0.45 ± 0.04	
1984 Mar 1		2.3 ± 0.1	1984 Mar 1	1.0 ± 0.2	
1984 Mar 25		1.3 ± 0.2	1984 Apr 21	0.54 ± 0.03	
1984 Mar 30		1.5 ± 0.2	1984 May 7	0.33 ± 0.04	
1984 Oct 23		0.56 ± 0.13	1984 May 20	0.29 ± 0.06	
1984 Oct 26		0.74 ± 0.10	1985 Mar 24	0.47 ± 0.07	
1984 Nov 19		0.53 ± 0.03	1985 Apr 11	0.5 ± 0.1	
1984 Nov 24		0.69 ± 0.04	1985 Jul 10	< 0.7 ^a	
1984 Nov 29		0.65 ± 0.04	1986 Feb 13	0.8 ± 0.1	
1985 Jan 15		1.0 ± 0.1	1986 Mar 19	19.7 ± 4.1	
1985 Jan 22		1.1 ± 0.1	1308+326.....	1982 Mar 18	0.7 ± 0.1
1985 Jan 26		1.6 ± 0.1	1982 Jun 20	0.37 ± 0.07	
1985 Feb 16		2.1 ± 0.1	1983 Mar 12	2.1 ± 0.3	
1985 Feb 19		1.5 ± 0.3	1983 May 13	2.0 ± 0.4	
1985 Mar 15		2.3 ± 0.3	1983 Jun 5	2.4 ± 0.4	
1985 Mar 18		2.5 ± 0.2	1983 Jul 6	0.9 ± 0.1	
1985 Mar 19	1.6 ± 0.2	1984 Jan 8	0.5 ± 0.1		
1985 Oct 15	2.2 ± 0.2	1984 Jan 29	0.7 ± 0.1		
1985 Nov 19	3.0 ± 0.2	1984 Feb 9	0.7 ± 0.1		
1985 Dec 11	3.4 ± 0.3	1984 Mar 1	0.7 ± 0.1		
1985 Dec 15	3.4 ± 0.3	1984 Mar 9	0.7 ± 0.1		
1985 Dec 17	3.5 ± 0.1	1984 Apr 5	0.7 ± 0.1		
1986 Jan 6	2.2 ± 0.2	1984 Apr 7	0.8 ± 0.1		
1986 Jan 12	2.6 ± 0.4	1984 May 20	0.5 ± 0.1		
1986 Jan 31	2.5 ± 0.2	1984 Jun 1	0.6 ± 0.1		
1986 Feb 3	2.3 ± 0.3	1985 Feb 16	0.9 ± 0.2		
1986 Mar 6	1.4 ± 0.1	1985 Mar 20	0.5 ± 0.1		
1986 Mar 31	1.5 ± 0.1	1985 Mar 24	0.6 ± 0.1		
0736+017.....	1982 Mar 17	1.2 ± 0.1	1985 Mar 26	0.6 ± 0.2	
	1982 Nov 24	0.7 ± 0.1	1985 Apr 17	0.4 ± 0.1	
	1982 Dec 18	1.0 ± 0.1	1985 Apr 18	0.40 ± 0.05	
	1983 Mar 3	1.1 ± 0.1	1985 Apr 23	0.42 ± 0.06	
	1984 Jan 8	1.3 ± 0.1	1985 May 15	0.34 ± 0.06	
	1984 Nov 19	1.6 ± 0.1	1985 May 17	0.48 ± 0.03	
	1985 Jan 22	2.3 ^b	1985 May 24	0.45 ± 0.06	
	1985 Feb 16	1.5 ± 0.1	1985 May 25	0.6 ± 0.1	

TABLE 8—Continued

Source	Date (U.T.)	B	Source	Date (U.T.)	B
	1985 Jun 19	0.7 ± 0.1	1921–293.....	1982 Sep 14	1.7 ± 0.5 ^a
	1985 Jun 20	0.5 ± 0.1		1982 Oct 10	1.6 ± 0.2
	1985 Jul 8	0.3 ± 0.1		1983 Aug 8	0.9 ± 0.1
	1985 Jul 17	0.75 ± 0.15		1983 Sep 28	1.1 ± 0.1
	1986 Feb 13	0.21 ± 0.03		1984 Apr 7	0.9 ± 0.2
	1986 Mar 18	0.20 ± 0.03		1984 Aug 28	<1.4
	1986 Apr 2	0.4 ± 0.1		1985 Jul 22	0.25 ± 0.02
	1986 Apr 11	0.3 ± 0.1		1985 Sep 9	0.5 ± 0.2
				1985 Oct 7	0.34 ± 0.04
1641+399.....	1982 May 17	3.2 ± 0.7	2200+420.....	1982 Aug 14	0.7 ± 0.1
	1982 Aug 14	3.7 ± 0.3		1982 Sep 14	1.0 ± 0.1
	1982 Oct 12	3.3 ± 0.5		1982 Dec 18	1.2 ± 0.2 ^c
	1983 Apr 13	2.3 ± 0.2		1983 Jun 11	1.0 ± 0.1
	1983 May 11	2.2 ± 0.6		1983 Jul 6	1.2 ± 0.2
	1983 May 12	2.2 ± 0.2 ^c		1983 Jul 9	1.2 ± 0.2
	1983 Jun 10	1.9 ± 0.2		1983 Aug 9	1.6 ± 0.2
	1983 Jul 5	1.8 ± 0.2		1983 Oct 1	2.2 ± 0.2
	1983 Jul 15	1.9 ± 0.3		1984 Apr 25	1.4 ± 0.1
	1983 Aug 10	1.7 ± 0.3 ^d		1984 Jun 2	1.6 ± 0.2
	1983 Sep 6	2.1 ± 0.3		1984 Oct 19	3.3 ± 0.7
	1983 Sep 31	1.7 ± 0.2		1984 Nov 25	3.1 ± 0.6
	1984 Apr 5	1.2 ± 0.2		1985 Jul 22	2.9 ± 0.5
	1984 Apr 25	1.3 ± 0.1		1985 Oct 8	3.3 ± 0.4
	1984 Jun 2	1.4 ± 0.2		1985 Oct 15	2.5 ± 0.3
	1985 Feb 19	1.22 ± 0.05		1985 Nov 6	1.9 ± 0.3
	1985 May 17	0.8 ± 0.1		1985 Nov 14	2.5 ± 0.6
	1985 May 25	0.9 ± 0.1	2223–052.....	1982 Sep 14	3.2 ± 0.5
	1985 Jun 24	0.7 ± 0.2		1983 Jul 12	0.6 ± 0.1
	1985 Jul 7	0.8 ± 0.1		1983 Aug 10	4.2 ± 0.8
	1985 Jul 24	0.9 ± 0.1		1983 Sep 5	1.9 ± 0.3
	1985 Sep 8	1.2 ± 0.2		1983 Oct 1	1.4 ± 0.2
	1985 Oct 15	1.0 ± 0.3		1984 May 31	0.44 ± 0.06
	1986 Apr 3	1.1 ± 0.1			
	1986 Apr 12	1.1 ± 0.1			

^a Poor plate.^b Eye estimate.^c $U: 1.5 \pm 0.1; V: 2.5 \pm 0.1$.^d $V: 1.8 \pm 0.1$.^e $U: 0.4 \pm 0.1; V: 3.0 \pm 0.3$.

the contribution from the violently variable components. An important item for future study will be to determine the relationship between the millimeter and the centimeter emission with good-quality frequency and temporal domain sampling.

7. Many OVV quasars exhibit an optical/ultraviolet excess over an extrapolation of the near-infrared continuum, particularly noticeable when the OVV quasar is in a low state. To illustrate this point, we present in Figure 3 near infrared to optical spectra for the sources at all epochs for which quasi-simultaneous (within <9 days) data are available. Four of the five BL Lac objects (0735+178, OJ 287, OV 236, and BL Lac) do not exhibit any excess in the optical at any epoch of observation. In contrast, 1308+326 does appear to exhibit a slight optical excess at one epoch, when very faint. However, three of the four OVV quasars (0736+017, 3C 279, and 3C 345) do exhibit a definite optical excess at most epochs of observation, this excess being particularly prominent when the OVV quasar concerned is in a low state.

In the case of the fourth quasar, 3C 446, we lack quasi-simultaneous near infrared to optical data when it is in a low state. However, as discussed in Brown *et al.* (1986), support for an excess being present is provided by the 1964 October *UBV* data of Sandage, Westphal, and Strittmatter (1966) when 3C 446 was very faint. They found that the spectrum was roughly

flat at 0.44–0.36 μm , suggesting that this OVV quasar also exhibits an optical excess when in a low state.

The spectral shape of the optical/ultraviolet excess observed in the spectra of 3C 345 and 0736+017 has been examined in detail (Bregman *et al.* 1986; Malkan and Moore 1986; Edelson and Malkan 1986) and has been shown to be similar to that of the “blue bump” exhibited by Seyfert 1 galaxies and low-polarization quasars. The blue bump has been attributed to a combination of Balmer continuum emission and thermal emission from an accretion disk of temperature 20,000–30,000 K (Malkan and Sargent 1982). An alternative explanation has been put forward by O’Dell, Scott, and Stein (1987), who suggest that the blue bump may be attributed to synchrotron emission from secondary electrons which result from pair creation consequent to inelastic collisions of relativistic protons with a dense ambient gas.

It is notable that to date no evidence for the presence of a blue bump has been found in the spectrum of a BL Lac object. For example, Moles *et al.* (1985) found that the optical continua of a sample of 17 BL Lac objects were well reproduced by power laws at all epochs of observation, and this was further confirmed by the *IUE* UV data from Ghisellini *et al.* (1986). Although our observations indicate that BL Lac objects which are in a low state may, on rare occasions, exhibit an optical/ultraviolet excess (e.g., 1308+326: Fig. 1*g*), this excess is small.

TABLE 9
METSAAHOVI MILLIMETER/CENTIMETRE FLUX DENSITIES (Jy)

SOURCE	DATE (U.T.)	WAVELENGTH		
		3.4 mm	8.1 mm	1.3 cm
0235 + 164.....	1985 Oct 24	2.03
	1986 Jan 10	...	1.37	...
	1986 Jan 16	1.52
	1986 Jan 18	...	1.49	1.49
	1986 Feb 11	...	1.61	...
	1986 Feb 17	...	1.44	...
	1986 Feb 20	1.57
0735 + 178.....	1986 Jan 10	...	1.07	...
	1986 Jan 16	1.46
	1986 Jan 18	..	1.12	...
	1986 Feb 1	...	1.24	...
	1986 Feb 14	...	1.12	...
	1986 Feb 19	1.35
	1986 Feb 25	...	1.14	...
1986 Apr 6	1.12	
0736 + 017.....	1986 Jan 10	...	1.63	...
	1986 Jan 17	2.39
	1986 Feb 25	...	1.57	...
0851 + 202.....	1985 May 18	6.64
	1985 Oct 24	5.36
	1986 Jan 11	...	3.97	...
	1986 Jan 17	4.27
	1986 Jan 18	...	3.96	...
	1986 Feb 6	...	4.86	...
	1986 Feb 7	4.41
	1986 Feb 11	...	5.36	...
	1986 Feb 15	4.74
	1986 Feb 20	...	6.08	...
	1986 Feb 21	5.19
	1986 Feb 24	...	6.52	...
	1986 Apr 7	7.21
1986 Apr 13	8.46	
1986 Apr 24	8.32	
1253 - 055.....	1985 May 19	4.77
	1985 Jul 15	3.72
	1986 Jan 17	...	8.24	...
	1986 Jan 18	8.50
	1986 Feb 3	8.61
	1986 Feb 4	...	8.38	...
	1986 Feb 22	8.50
1986 Apr 8	7.42	
1308 + 326.....	1985 May 16	2.59
	1986 Jan 17	2.25
	1986 Jan 19	...	2.04	...
	1986 Feb 3	2.47
	1986 Feb 4	...	2.05	...
	1986 Feb 9	...	2.06	...
	1986 Feb 25	2.28
	1986 Apr 5	1.58
1986 Apr 13	1.44	
1641 + 399.....	1985 May 17	5.20
	1985 Oct 20	6.60
	1986 Jan 10	...	8.99	...
	1986 Jan 17	10.41
	1986 Jan 18	10.63
	1986 Jan 19	...	9.18	...
	1986 Feb 3	11.02
	1986 Feb 4	...	9.72	...
	1986 Feb 10	...	9.29	...
	1986 Feb 17	...	9.03	...
	1986 Feb 26	10.71
	1986 Apr 8	6.25
	1986 Apr 13	6.80
1986 Apr 23	6.04	

TABLE 9—Continued

SOURCE	DATE (U.T.)	WAVELENGTH		
		3.4 mm	8.1 mm	1.3 cm
2200+420.....	1985 Aug 14	1.09
	1985 Aug 30	1.69
	1985 Oct 24	1.29
	1985 Dec 1	1.28
	1986 Feb 2	...	1.68	...
	1986 Feb 11	...	1.66	1.68
	1986 Feb 17	...	1.72	...
	1986 Feb 19	1.60
	1986 Feb 25	...	2.05	...
	1986 Apr 8	1.59
2223-052.....	1986 Jan 11	...	3.36	...
	1986 Jan 17	3.67
Flux uncertainties		0.30	0.20	0.20

8. The X-ray spectra often exhibit an excess over an extrapolation of the near-infrared/ultraviolet continuum with a flatter spectral slope (e.g., 3C 446: Fig. 1*k*). However, the spectrum of OJ 287 presented here (Fig. 1*e*) is consistent with a continuation of the near-infrared to ultraviolet continuum, with some spectral steepening occurring between the near-infrared/ultraviolet and X-ray wavelength regimes. Marashi *et al.* (1986) discuss X-ray properties of blazars in detail, however, our samples contain only two common sources.

The combination of spectral properties of 1–4 listed above indicates that the centimeter to ultraviolet emission of blazars originates from at least two synchrotron components. Self absorption of the synchrotron flux occurs at low frequencies, while radiative energy losses affect the electrons at high frequencies, resulting in the observed spectral steepening. The high-frequency cutoff which is sometimes observed can be attributed to a high-energy cutoff in the electron energy distribution. Additional evidence for the synchrotron origins of the centimeter to ultraviolet flux is provided by the high polarization and violent variability seen throughout this wavelength region. The flux variations can be understood in terms of recurrent injections/reaccelerations of the emitting electrons with subsequent radiative decay (see also Paper II). The optical/ultraviolet excesses seen in the spectra of blazars, particularly when they are in a low state, are indicative of one or more separate (and probably nonsynchrotron) emission components which may be concealed when the violently variable “flaring” emission is in a high state.

The 1984 February X-ray spectrum of OJ 287 shown in Figure 1*e* appears to be the high-frequency tail of the variable millimeter-optical synchrotron spectrum, while the X-ray spectra of 3C 446 and 3C 279 are consistent with inverse Compton emission from the electrons responsible for the synchrotron radiation. In particular, the X-ray spectral slope of roughly -0.8 observed in 3C 446 is in agreement with the slope of -0.75 expected from a population of relativistic electrons of power-law energy distribution $N(E) = KE^{-2.5}$. We shall show in § IV*b* that the near-infrared to ultraviolet spectra of the blazars are indicative of such an electron energy distribution.

b) Spectral Indices in the Far-Infrared to Ultraviolet

The spectral index of a power-law spectrum is given by $d(\log F_\nu)/d(\log \nu)$ and corresponds to the slope of the spectrum on a log flux density versus log frequency plot. In Table 10 are

presented the maximum, minimum, and mean spectral indices for each source obtained from our data set for (a) the far/mid-infrared (~ 10 – $1100 \mu\text{m}$), (b) the near-infrared (~ 1 – $5 \mu\text{m}$), (c) the optical, and (d) the ultraviolet wavelength regions. Of course, the maximum and minimum spectral indices shown can, strictly speaking, be regarded only as lower and upper limits, respectively; however, Table 10 demonstrates some very interesting trends for the spectral slopes of the blazars *as a class* in the various wavelength regions.

1. The mean spectral slope observed in the near-infrared wavelength region is steeper than that observed in the far/mid-infrared. This result reflects the presence of the mid/near-infrared spectral break noted previously. In the near-infrared to ultraviolet the mean spectral slope generally exhibits further steepening, except for those sources whose spectra show evidence for an optical/ultraviolet excess (see number 4 below).

2. In the far/mid-infrared, the maximum and minimum spectral indices, α_{max} and α_{min} , observed for the whole sample are approximately -0.7 and approximately -1.4 , respectively.

3. In the near-infrared, α_{max} for the sample is again roughly -0.7 but α_{min} is steeper than that observed in the far/mid-infrared at roughly -1.9 .

4. As noted previously, the spectra of OVV quasars in general exhibit an optical/ultraviolet excess over an extrapolation of the near-infrared spectrum. The optical spectra of OVV quasars which are in a low state are *not* well fitted by power laws, and the derived spectral indices are significantly flatter than those obtained when the quasars are brighter. Thus for these sources it is difficult to derive the optical spectral slope of the power law synchrotron emission. If we consider the BL Lac objects only, the value obtained for α_{max} in the optical is roughly -0.7 , the same as observed at lower frequencies.

The sources for which the steepest observed spectral slope coincides with rapid spectral curvature suggestive of a high-frequency cutoff are indicated in Table 10. If we exclude these sources, we obtain a value for α_{min} of roughly -2.2 in the optical, similar to the value obtained in the near-infrared. (Note: the source for which the greatest number of measurements of the optical spectral index have been obtained, 1308+326 [33 observations taken from a histogram presented in Mufson *et al.* 1985] virtually spans the range in optical spectral index displayed by the sample as a whole, with $-2.0 < \alpha < -0.7$.)

5. In the ultraviolet α_{max} is roughly -0.8 , similar to the value obtained at longer wavelengths. α_{min} is approximately

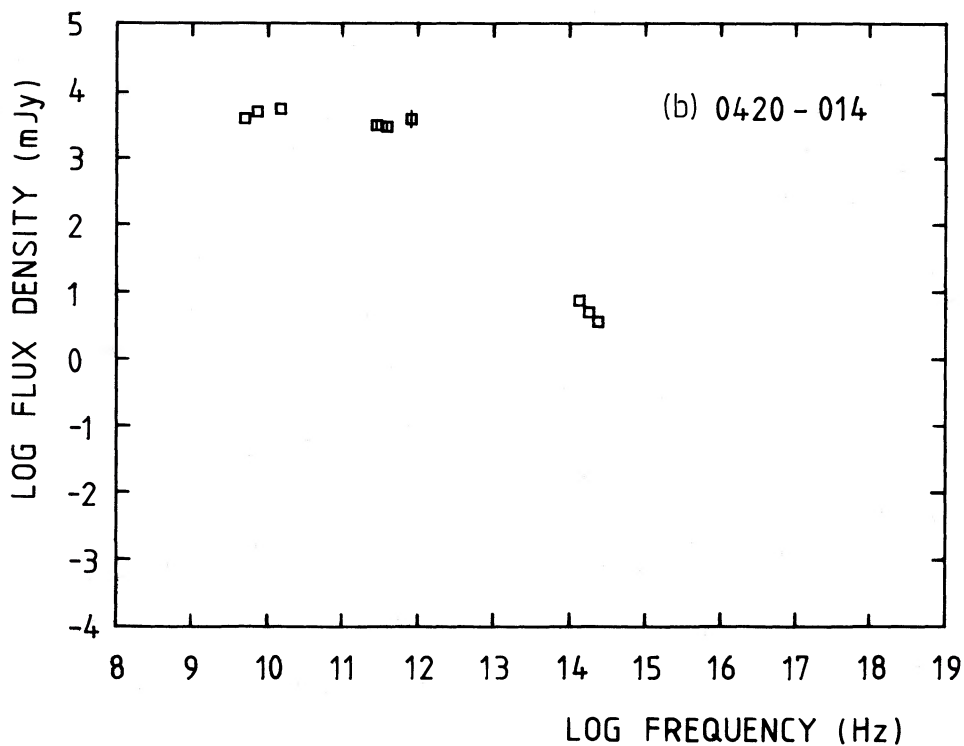
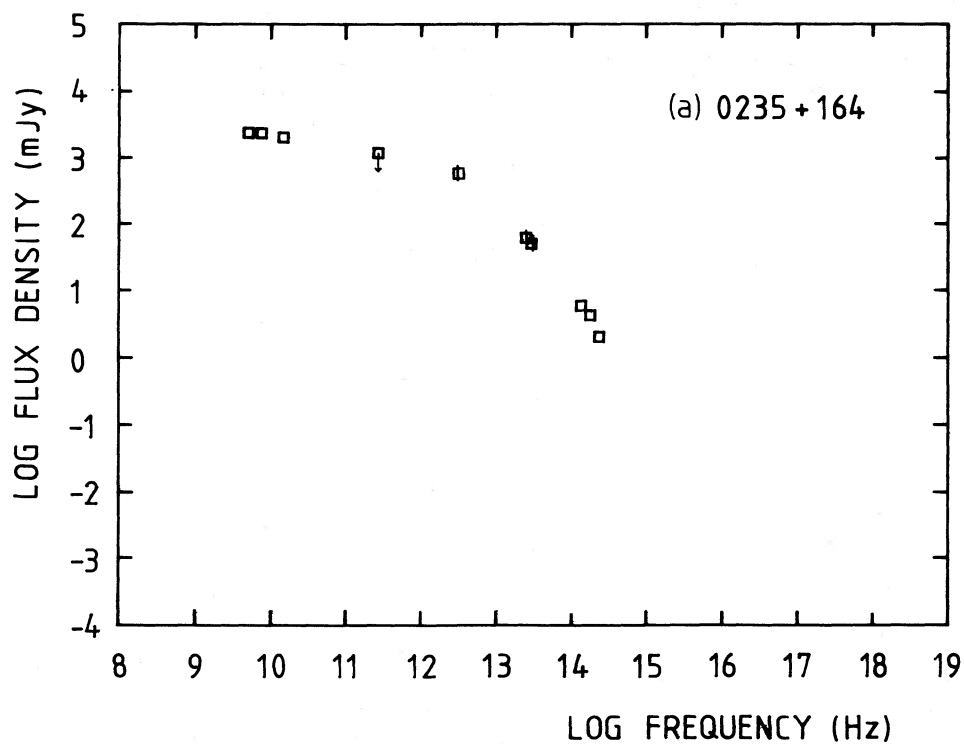


FIG. 1.—(a–k) Quasi-simultaneous multifrequency spectra of 11 blazars. Error bars are shown where the observational uncertainties exceed 10%. The epochs of observations are: 0235, 1983 August; 0420, 1983 March; 0735, 1983 September; 0736, 1983 March; OJ 287, 1984 February; 3C 279, 1984 February; 1308, 1986 February; 3C 345, 1983 September; OV 236, 1983 August; BL Lac, 1983 August; 3C 446, 1983 November.

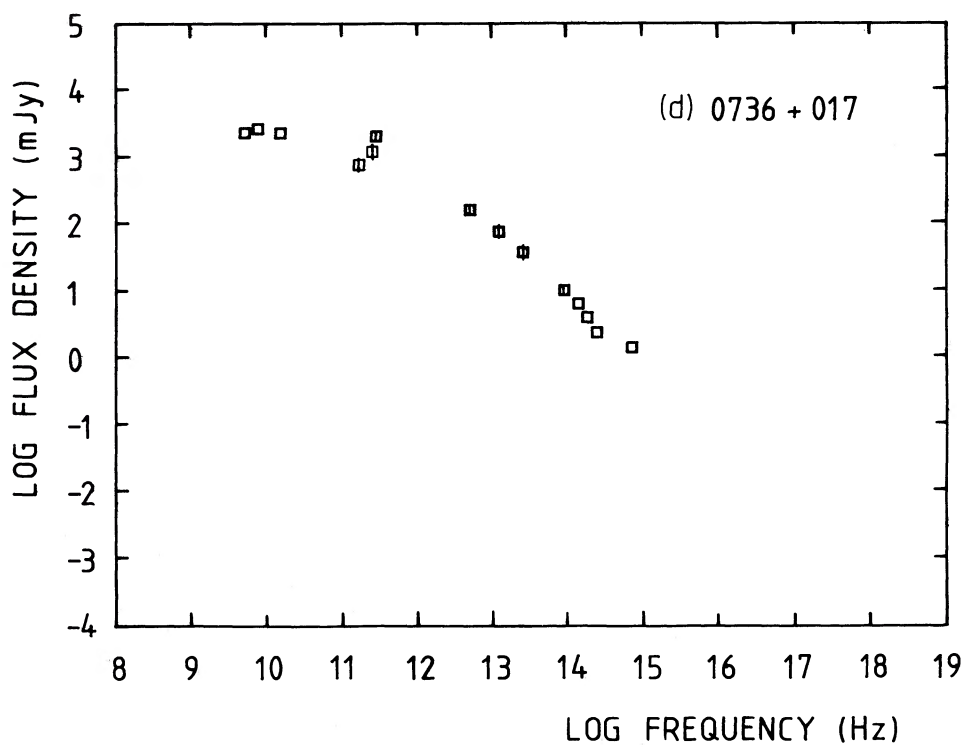
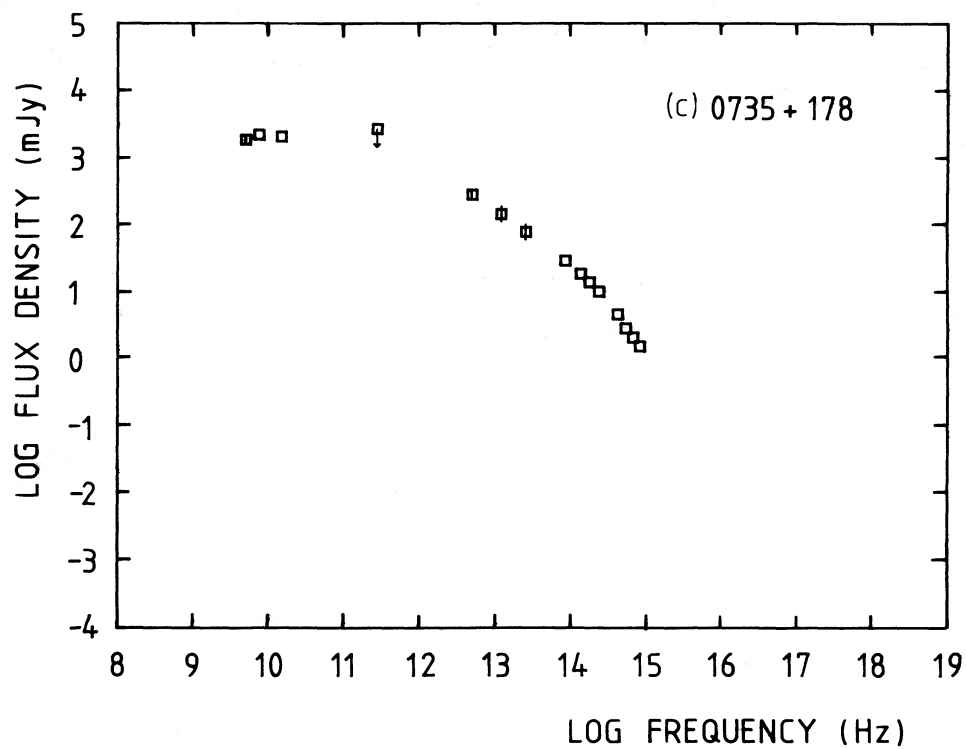


FIG. 1—Continued

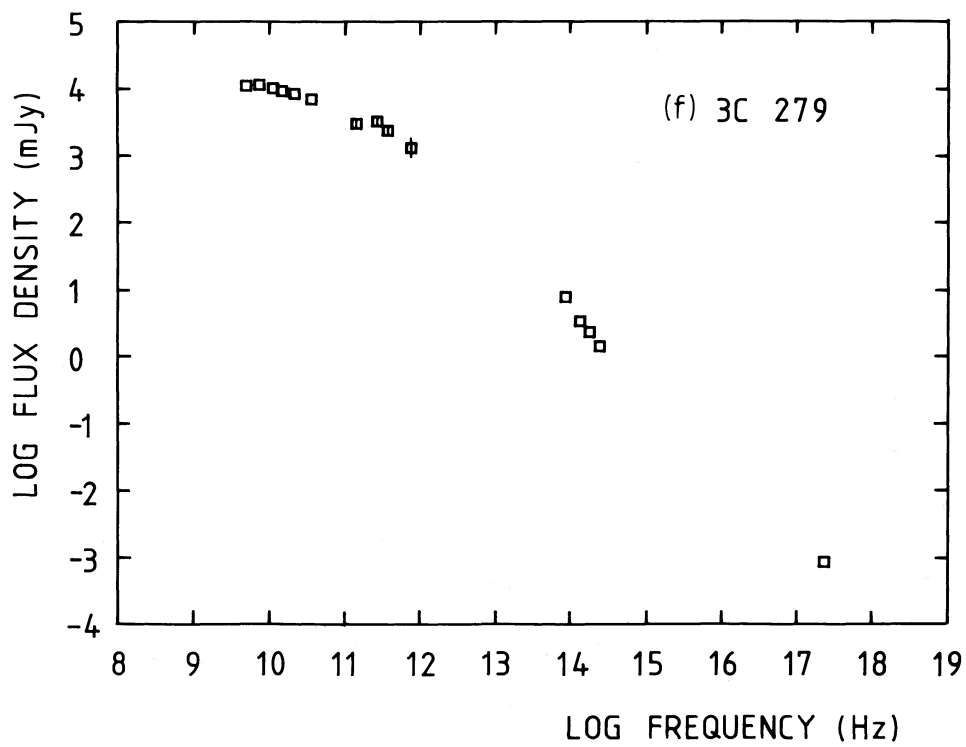
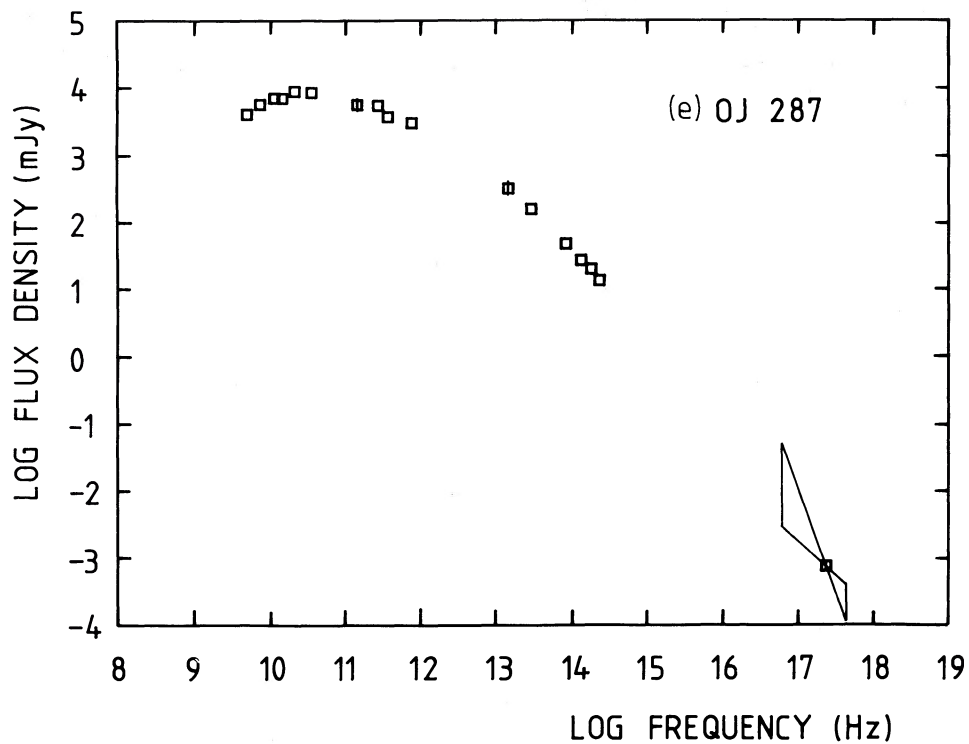


FIG. 1—Continued

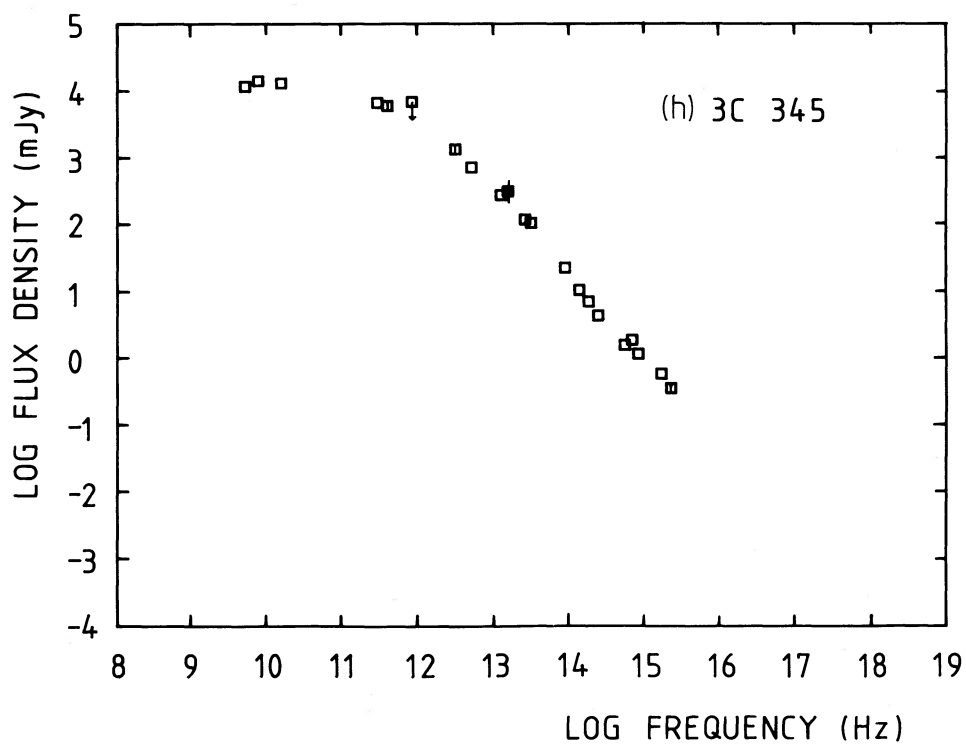
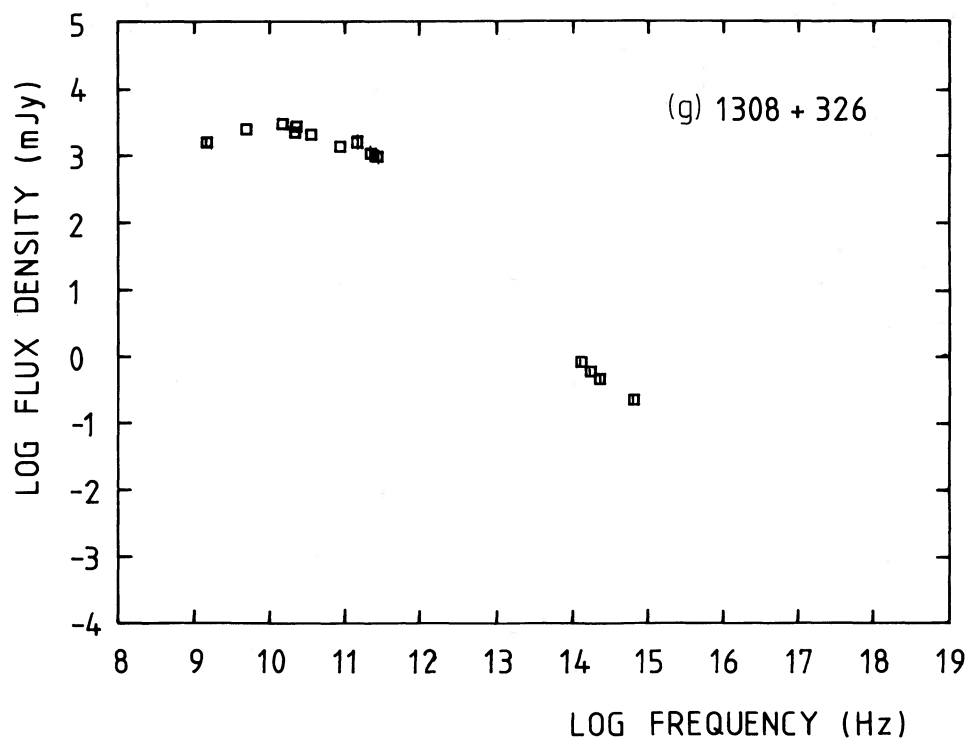


FIG. 1—Continued

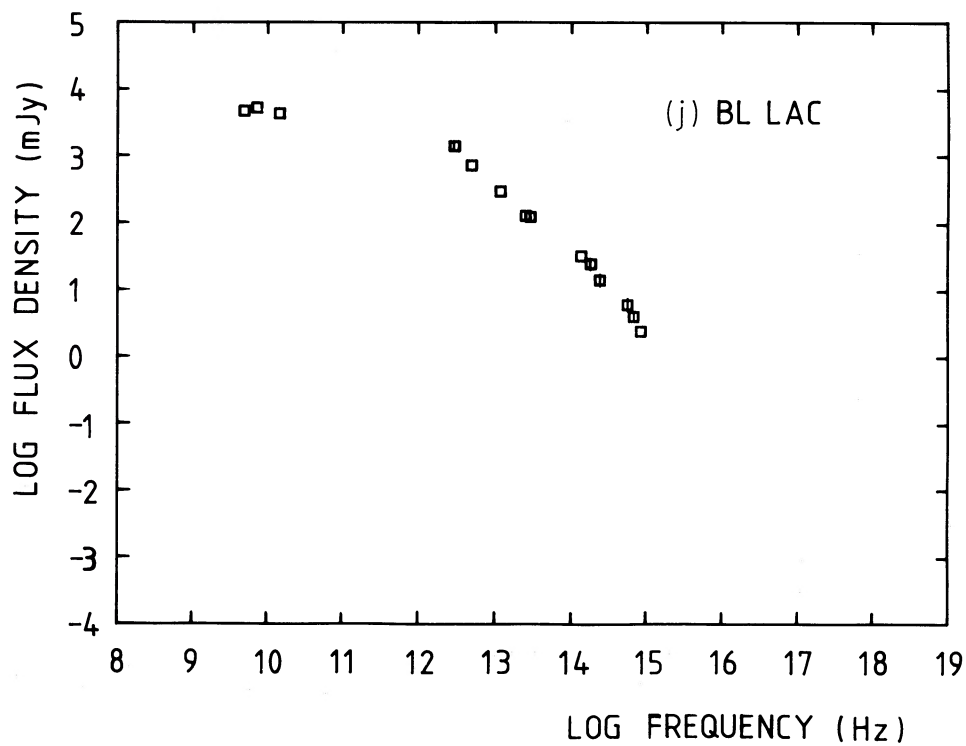
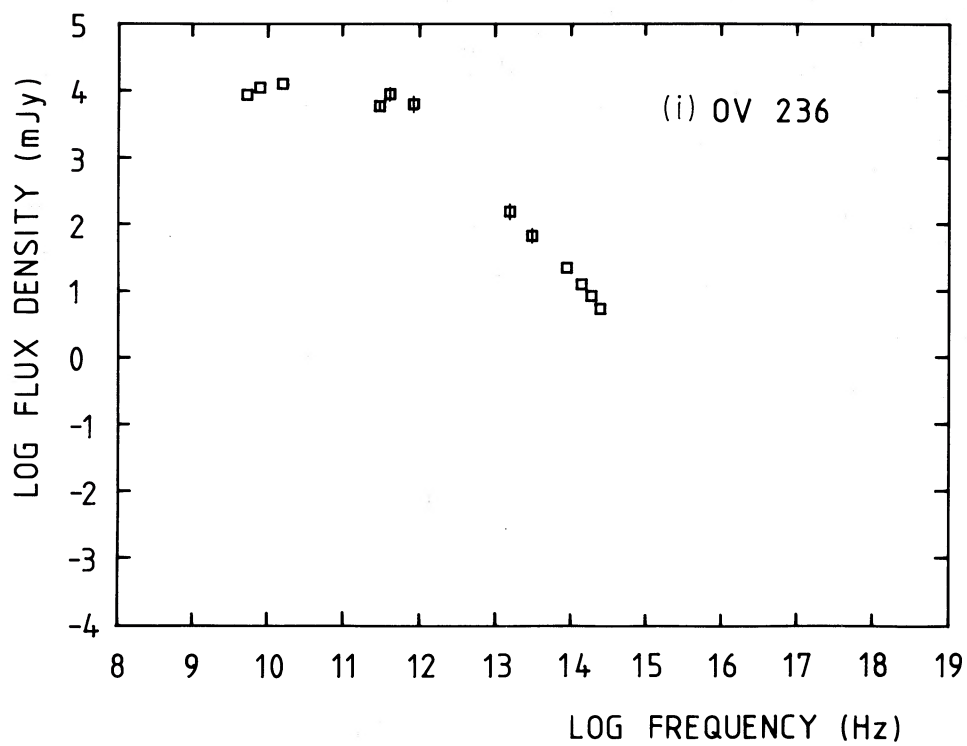


FIG. 1—Continued

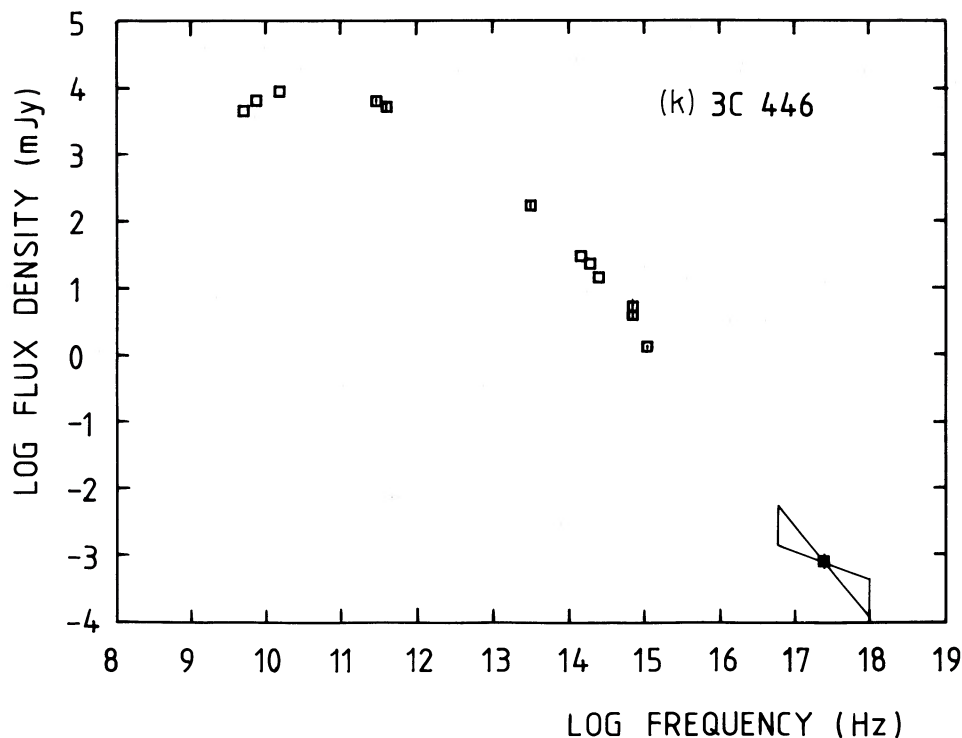
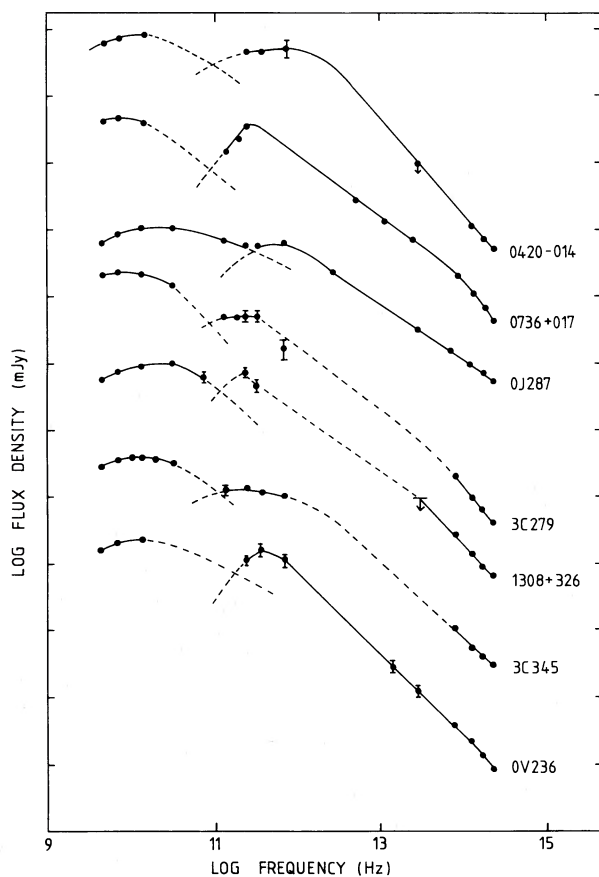


FIG. 1—Continued



–2.2, similar to the values obtained in the near-infrared and optical wavelength regions.

V. INTERPRETATION

Our results suggest that the emission from blazars can be understood in terms of a multicomponent model:

- (1) a “quiescent” emission component, which dominates the centimeter emission, the variation of which is responsible for the long-term (roughly of years) variations observed at these wavelengths. This component extends to shorter wavelengths where it is masked by component 2;
- (2) a violently variable “flaring” emission component which dominates the millimeter to ultraviolet emission, and which rises and decays on a time scale roughly of days to weeks;
- (3) an additional emission component which is possibly thermal in origin and is observed in the optical/ultraviolet spectra of OVV quasars.

As discussed in Papers I and II, there is convincing evidence in favor of relativistic beaming in blazars. The fact that VLBI maps show the presence of jet-like structures in superluminal sources has led to a growing consensus that these VLBI structures reveal the orientation of a relativistic jet which is directed

FIG. 2.—Spectra of nine blazars for which we have quasi-simultaneous centimeter through infrared data. The separate centimeter component is clearly visible for most of the sources. Error bars are shown when the observational uncertainties exceed 10% and the ordinate is labeled in factors of 10. Observations dates were 0420, 1983 March; 0736, 1983 April; OJ 287, 1983 April; 3C 279, 1983 March; 1308, 1984 February; 3C 345, 1983 April; OV 236, 1984 August. Dashed line shows a reasonable extrapolation from otherwise well sampled data in frequency space.

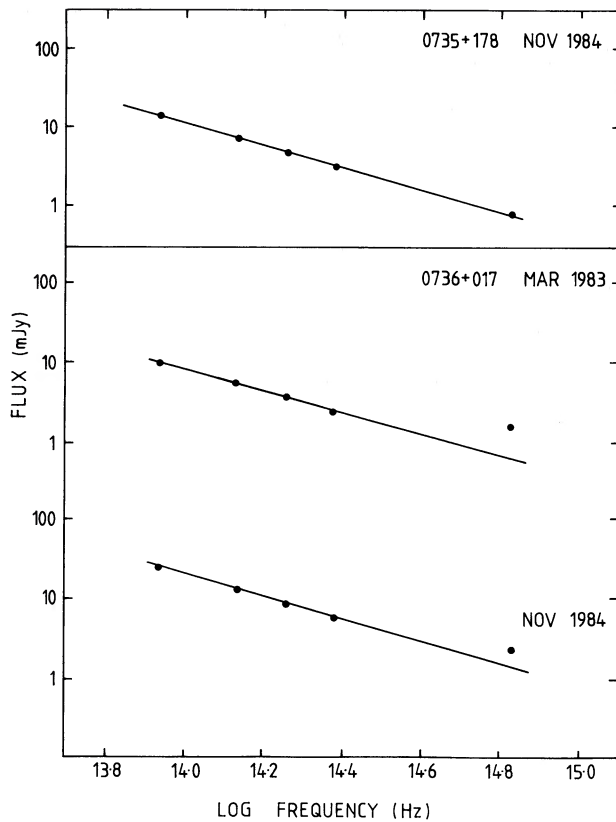


FIG. 3a

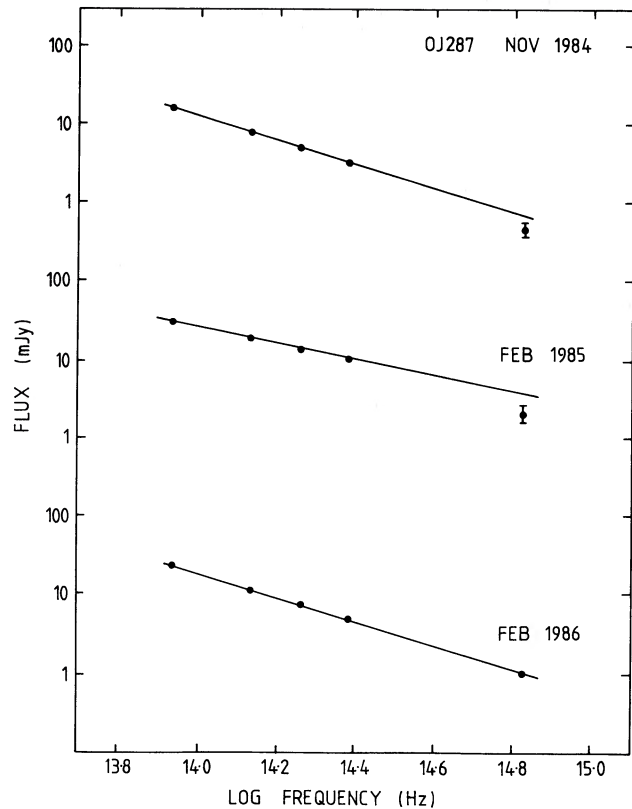


FIG. 3b

FIG. 3.—(a-f) Quasi-simultaneous near-infrared to optical spectra of nine blazars. The optical excess over a power law extrapolated from the infrared can be clearly seen in the case of the OVV quasars 0736, 3C 345, and 3C 279 when they are in a low state. The BL Lac object 1308 may represent an intermediate case. Error bars are shown where the observational uncertainties exceed 10%.

toward the observer and which is responsible for the observed beaming.

Recent polarization measurements of compact radio sources indicate that the magnetic fields are largely turbulent (Jones *et al.* 1985). OJ 287, 3C 345, BL Lac, and 3C 454.3, however, show clear evidence for a net magnetic field direction in the compact “core” aligned orthogonal to the direction of the observed VLBI structures and thus to the axis of the inferred relativistic jet (Jones *et al.* 1985; Brindle *et al.* 1986). BL Lac appears to develop orthogonal fields during some outbursts, a phenomenon which Jones *et al.* (1985) suggest may result from shock compression of the magnetic field.

This evidence suggests a scenario where the quiescent emission component is identified with emission from the bulk of a relativistic jet aligned close to the line of sight, while the flaring components arise in smaller regions of enhanced emission within the jet which result from local injections or reaccelerations of the emitting electrons. [Reacceleration of electrons could be the result of the passage of a shock through the jet (see, e.g., Marscher and Gear 1985).]

a) Centimeter Emission

The centimeter to near-infrared spectra shown in Figure 1 of two sources, 3C 345 and BL Lac, are consistent with a single emission component with a slow turnover due to self-absorption occurring at millimeter to centimeter wavelengths. However, as discussed in § IV, the centimeter emission in general exhibits an excess over an extrapolation of the milli-

meter spectrum and a turnover at $\sim 2\text{--}5$ cm, strongly suggestive of the presence of an additional spectral component which dominates the centimeter emission. Due to the violent variability of the blazars, it is not surprising that this “quiescent” component is rarely, if ever, observed at millimeter to ultraviolet wavelengths.

b) Millimeter-Ultraviolet Emission

We can compare the range of the spectral index α observed in the various wavelength regions above the spectral turnover with theoretical predictions of the value of α for optically thin synchrotron emission from a population of relativistic electrons of power-law energy distribution $N(E) = KE^{-s}$. The “canonical” value of s , corresponding to that deduced for many galactic and extragalactic sources, is ~ 2.5 . The spectral slope of optically thin synchrotron emission from such a population of electrons, whose energy distribution is unmodified by energy losses, is $(1 - s)/2 \approx -0.75$. This slope is in agreement with the *flattest* slopes observed at far-infrared to ultraviolet wavelengths (apart from the slopes derived for the optical/ultraviolet spectra of OVV quasars which exhibit a “blue bump”).

If the electrons lose energy radiatively while experiencing continuous injection into, or reacceleration in, a magnetic field, then at low frequencies, where energy losses are not important, the spectral slope is roughly -0.75 . Above a break frequency ν_b , radiation losses steepen the spectrum to a slope of $-s/2 \approx -1.25$ (Kardashev 1962). Alternatively, if the electrons

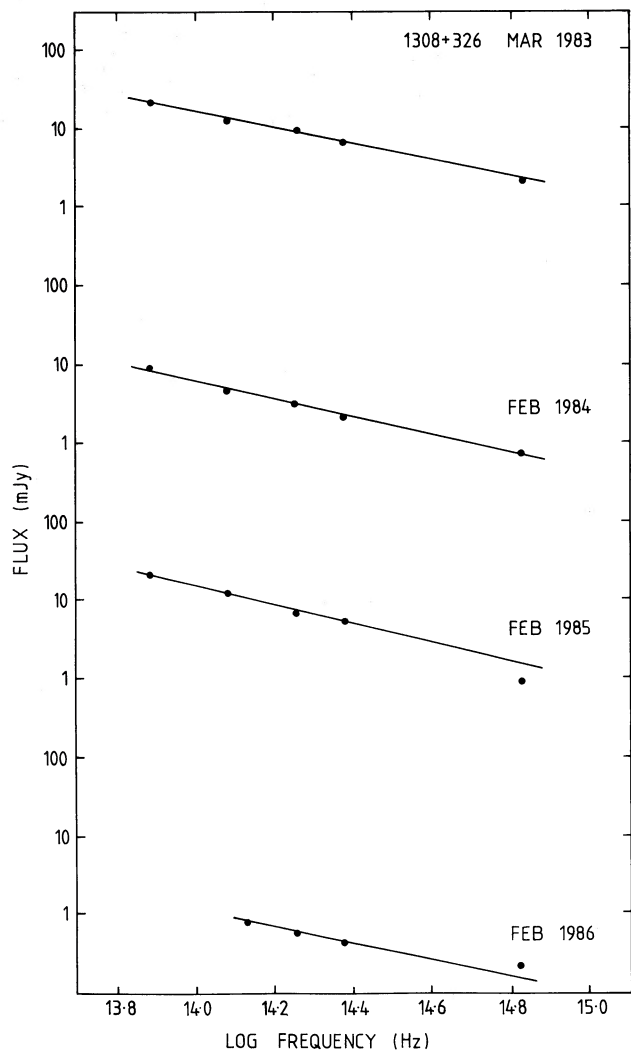


FIG. 3c

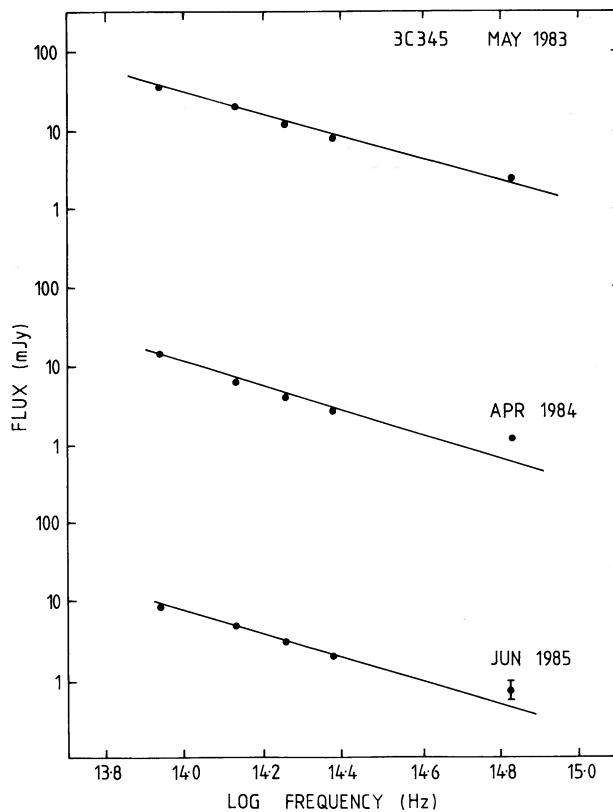


FIG. 3d

experience an instantaneous burst of injection or reacceleration, and subsequently lose energy radiatively, the spectrum steepens at a break frequency ν'_b from its initial slope of $(1-s)/2$ to a slope of $-(2s+1)/3 \approx -2$ (Kardashev 1962).

If we attribute the flare events which are seen in the emission of blazars to repeated injections/reaccelerations of the emitting electrons which subsequently decay radiatively (see also Paper II), the spectral index of the optically thin flux would be expected to vary between approximately -0.75 and approximately -2 . In the absence of a high-frequency cutoff, this range of spectral index is indeed observed at near-infrared to ultraviolet wavelengths. If a high-energy cutoff occurs in the electron energy distribution, a high-frequency cutoff is observed in the spectrum, and in this case, of course, α_{\min} is steeper than -2 .

The minimum spectral slope in the far/mid-infrared is flatter than -2 . We attribute this to the longer electron lifetimes in this wavelength region (see below). A new flare is likely to occur before the far/mid-infrared spectral slope has steepened to -2 , with the emission from the new component subsequently dominating the spectrum.

Obviously, variability studies are required to understand

more fully the emission mechanisms of blazars. However, the quasi-simultaneous spectra do suggest strongly that the behavior of the optically thin violently variable millimeter/submillimeter to near-infrared emission of blazars can be explained in terms of simple synchrotron theory, ruling out any necessity for the introduction of more exotic emission mechanisms.

The fact that the infrared to ultraviolet fluxes of blazars are seen to vary together on a time scale of days to weeks (see, e.g., Paper II; Holmes *et al.* 1984) indicates that the flaring regions are small ($r \approx 10^{-3}$ – 10^{-2} pc), where r is approximately the radius of the flaring region. There is in general evidence for a smooth radial dependence of the magnetic field B and electron number density n_e in these regions; however, since the regions are small we shall use the slab-geometry approximation of Burbidge, Jones, and O'Dell (1974). As pointed out by Bregman *et al.* (1984), the slab model is useful even when the approximation of homogeneity is not valid, as it provides average values of the magnetic field and electron number density, weighted by the regions of plasma which contribute most strongly to the emission.

We follow the method of Paper I to obtain approximate

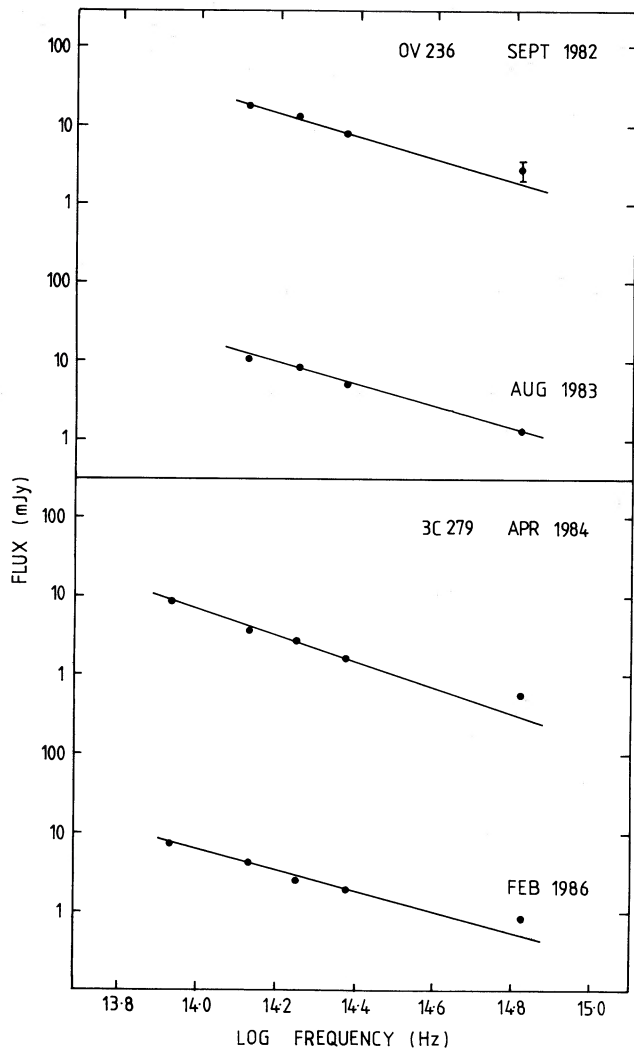


FIG. 3e

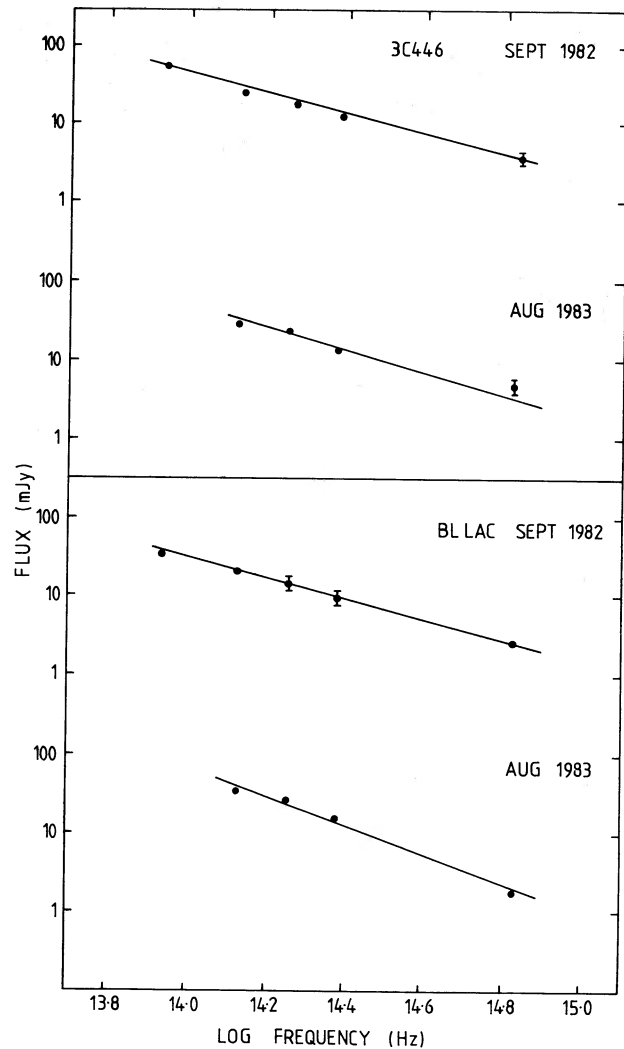


FIG. 3f

values for r for our sample of blazars and use the slab approximation to obtain estimates for B . Table 11 presents values for r and B , calculated for the quasi-simultaneous spectra presented in § II. We have assumed that the mean angle θ between B and the line of sight to the observer is $\sim \pi/2$; this assumption is valid if the magnetic field is largely turbulent, as suggested by the observational evidence (Jones *et al.* 1985).

Table 11 shows that typically $r \sim 10^{13} - 10^{15}$ m ($\sim 10^{-3} - 10^{-1}$ pc) and $B \sim 1$ G. Thus the flaring regions are small, as indicated by the variability time scale, with strong magnetic fields.

Again following the methods set out in Paper I, we can also obtain estimates for the magnetic, photon, and particle energy densities, $u(m)$, $u(ph)$, and $u(e)$. Estimate $u(e)$ depends on the characteristic Lorentz factor γ_l of the relativistic electrons radiating at the low-frequency cutoff, ν_l , which is not directly observable. However, it is possible to restrict the possible range of $u(e)$ since Wardle (1977) set a lower limit of ~ 50 on γ_l and, in addition, $\gamma_l < \gamma_m$, where γ_m is the characteristic Lorentz factor of the electrons radiating at the turnover frequency ν_m [$u(e)$ is not very sensitively dependent on γ_l ; a change in γ_l from 50 to 200 results in a reduction of $u(e)$ by only a factor of ~ 2].

Values of $u(m)$ and $u(ph)$ and the possible range of $u(e)$ have been estimated for each of our quasi-simultaneous spectra and the results are presented in Table 12. The uncertainties involved in this analysis are large. In particular, $u(ph)$ is quite sensitively dependent on the bulk Doppler factor \mathcal{D} of the emitting electrons, for which we assume a value of 5 (see Paper I; Madau, Ghisellini, and Persic 1986). Should $\mathcal{D} \sim 5$ not be a good assumption, $u(ph)$ may differ by up to one order of magnitude from the value obtained here. In addition, should the assumption of $\theta \sim \pi/2$ not be valid, the value of B may also be greater than that obtained here by up to one order of magnitude. However, it does seem clear that the relativistic electrons dominate the energy density of the flaring regions [$u(e) > u(m)$, $u(ph)$], although the dominance is not as overwhelming as is indicated for more extended regions (see, e.g., Burbidge *et al.* 1974). In addition, our results indicate that probably $u(ph) > u(m)$: thus inverse Compton radiation is a very important, possibly the dominant, energy loss mechanism in these regions.

Given $u(m)$ and $u(ph)$, it is possible to estimate ν_b , the break frequency expected a time T after the commencement of a flare, by assuming that the radiative cooling time of the electrons

TABLE 10
MAXIMUM, MINIMUM, AND MEAN SPECTRAL INDICES IN THE FAR-INFRARED TO ULTRAVIOLET^a

Source	Far/Mid-IR	Near-IR	Optical	UV
0235 + 164:				
Maximum	-0.74 ± 0.04	-1.25 ± 0.03 ^b	-2.9 ± 0.1 ^b	...
Minimum	-1.0 ± 0.2	-1.8 ± 0.1	-4.8 ± 0.1 ^b	...
Mean	-0.9(6)	-1.6(6)	-3.9(7)	...
0420 - 014:				
Maximum	-1.23 ± 0.04	-1.0 ± 0.1
Minimum	-1.3 ± 0.2	-1.3 ± 0.1
Mean	-1.2(2)	-1.1(2)
0735 + 178:				
Maximum	-0.7 ± 0.2	-0.7 ± 0.3	-1.5 ± 0.1
Minimum	-1.5 ± 0.1	-3.3 ± 0.1 ^b	-2.0 ± 0.2
Mean	-0.77 ± 0.05 ^c	-1.2(9)	-1.7(14)	-1.7(4)
0736 + 017:				
Maximum	-1.2 ± 0.1	-0.5 ± 0.1 ^d	...
Minimum	-1.7 ± 0.1	-1.6 ± 0.1 ^d	-1.8 ± 0.1 ^e
Mean	-0.88 ± 0.05 ^c	-1.4(6)	-0.9(4)	...
0851 + 202:				
Maximum	-0.7 ± 0.1	-0.7 ± 0.1	-1.1 ± 0.1	-0.8 ± 0.1
Minimum	-1.0 ± 0.1	-1.6 ± 0.1	-1.8 ± 0.2	-1.9 ± 0.1
Mean	-0.85(7)	-1.2(20)	-1.3(29)	-1.4(13)
1253 - 055:				
Maximum	0.9 ± 0.3	-1.3 ± 0.1
Minimum	-1.1 ± 0.1	-1.9 ± 0.1
Mean	-1.0(2)	-1.7(9)	-0.6 ± 0.1 ^{c, d}	...
1308 + 326:				
Maximum	-1.1 ± 0.1	~ -0.7 ^e	...
Minimum	-1.5 ± 0.1	~ -2.0 ^e	...
Mean	-0.9 ± 0.1 ^c	-1.7(9)	~ -1.3 ^c (33)	...
1641 + 399:				
Maximum	-0.8 ± 0.1	-1.05 ± 0.02	-0.8 ± 0.1 ^d	-1.2 ± 0.1 ^d
Minimum	-1.06 ± 0.04	-1.74 ± 0.05	-1.5 ± 0.1 ^d	-2.1 ± 0.2
Mean	-0.95(7)	-1.5(19)	-1.2(4)	-1.8(6)
1921 - 293:				
Maximum	-1.3 ± 0.1
Minimum	-1.5 ± 0.1
Mean	-1.18 ± 0.04 ^b	-1.4(3)
2200 + 420:				
Maximum	-0.8 ± 0.1	...	-1.6 ± 0.2	...
Minimum	-0.9 ± 0.1	...	-2.2 ± 0.2	...
Mean	-0.8(3)	-0.9 ^f (6)	-2.0(4)	...
2223 - 052:				
Maximum	-0.76 ± 0.03	-1.22 ± 0.03	-0.5 ± 0.2	-1.7 ± 0.3
Minimum	-1.1 ± 0.1	-1.9 ± 0.1	-2.1 ± 0.3	-2.2 ± 0.4
Mean	-0.9(4)	-1.6(8)	-1.5(11)	-2.1(4)

^a At least three data points have been used to calculate each spectral index. The number of epochs of observation used to derive the maximum, minimum and mean spectral indices is shown in brackets after the mean.

^b Spectral curvature present.

^c Spectral index available for one epoch only.

^d Shows an optical/UV "bump."

^e Taken from a histogram presented in Mufson *et al.* 1985.

^f All the near-infrared observations of BL Lac are consistent with this spectral slope.

which radiate predominantly at ν_b is $\sim T$.

$$\nu_b(\text{Hz}) \sim 4 \times 10^{15} [u(m) + u(\text{ph})]^{-2} \frac{B\mathcal{D}}{(1+z)} T^{-2}, \quad (1)$$

where T is measured in seconds, B in G, and $u(m)$ and $u(\text{ph})$ in J m^{-3} . The values for $u(m)$ and $u(\text{ph})$ shown in Table 12 indicate values for ν_b of $\sim 10^{11}$ – 10^{14} Hz and $\sim 10^{10}$ – 10^{13} Hz expected 1 week and 4 weeks, respectively, after the commencement of a flare. Equation (1) is valid in the case of continuous injection or

reacceleration of electrons (see Kardashev 1962). Observations of blazars indicate that prolonged injection/reacceleration of electrons can take place over a period of up to ~ 3 –4 months (see e.g., Glassgold *et al.* 1983; Barbieri *et al.* 1985). If, however, the injection/reacceleration were to cease after a few days, ν_b would evolve to lower frequencies somewhat faster than suggested by equation (1).

As discussed in § III, a spectral turnover/flattening, attributable to self-absorption of the synchrotron flux, is generally

TABLE 11

ESTIMATED SIZES AND MAGNETIC FIELDS FOR THE FLARING REGIONS OF BLAZARS

Source	r ($\times 10^{14}$ m)	B (G)
0235+164.....	0.7	1.4
0420-014.....	1.8	1.0
0735+178.....	2.4	0.5
0736+017.....	1.1	0.6
0851+202.....	3.0	0.5
1253-055.....	12	0.2
1308+326.....	3.7	0.4
1641+399.....	4.1	0.6
1921-293.....	2.8	0.7
2200+420.....	0.2	1.5
2223-052.....	20	0.2

observed in the spectra of blazars at $\sim 10^{11}$ – 10^{12} Hz. For sources in which $\nu_b < \nu_m$, we might expect the entire submillimeter to optical spectrum to exhibit a slope consistent with emission from electrons whose energy distribution is steepened by radiative energy losses ($\alpha \lesssim -1.2$).

Spectral breaks are indeed often observed in the spectra of blazars between $\sim 10^{12}$ and 10^{14} Hz. In addition, the submillimeter to optical spectra of those sources which show no evidence for a mid-near-infrared spectral break do generally exhibit spectral slopes of approximately -1.2 , suggesting that $\nu_b < \nu_m$. The rough agreement between these observational results and the range of values we have calculated for ν_b is encouraging, supporting the conclusion that the submillimeter to ultraviolet emission of blazars is synchrotron emission from a single, compact component and suggesting that the values which have been estimated for $u(m)$ and $u(ph)$ are reasonably close to the true values. Thus the slab-geometry approximation appears to yield a reasonable description of the conditions prevailing in the flaring regions of blazars.

Using the method of Marscher and Gear (1985), we obtain cooling times of less than a few days at $3 \mu\text{m}$ and roughly weeks at $100 \mu\text{m}$, for both the synchrotron and the inverse Compton emission. These derived time scales support a scenario where the near-infrared to ultraviolet emission can exhibit significant decay and spectral steepening between flare events occurring once every 1–3 months, while the far/mid-infrared emission exhibits more modest variability.

Of the quasi-simultaneous spectra presented in this paper, only two sources, 0736+017 and OV 236, exhibit submillimeter/millimeter spectral slopes which approach the optically thick slope of 2.5 expected from a homogeneous synchrotron source. For the most part the blazars exhibit relatively flat submillimeter/millimeter spectral indices of ~ 0 – 0.6 . (Subtraction of a possible underlying component which becomes self-absorbed at centimeter wavelengths and has an optically thin spectral slope of approximately -0.75 does not in general result in appreciable steepening of the optically thick spectral index.) Flattening of the optically thick spectrum can result from inhomogeneity in the magnetic field and particle density of the emission region or the occurrence of continuous injection/reacceleration of the emitting electrons, or both (Paper I; Marscher and Gear 1985; Peterson and Dent 1973).

TABLE 12

ESTIMATED ENERGY DENSITIES FOR THE FLARING REGIONS OF BLAZARS

Source	$u(m)$ ($\times 10^{-3}$ J/m $^{-3}$)	$u(ph)$ ($\times 10^{-3}$ J/m $^{-3}$)	$u(e)$ ($\times 10^{-3}$ J/m $^{-3}$)
0235+164.....	0.1	3.0	60 $< u(e) < 1100$
0420-014.....	0.04	1.4	20 $< u(e) < 380$
0735+178.....	0.01	0.1	1.3 $< u(e) < 20$
0736+017.....	0.01	0.1	1.2 $< u(e) < 15$
0851+202.....	0.01	0.06	0.6 $< u(e) < 9$
1253-055.....	0.001	0.01	0.2 $< u(e) < 2.3$
1308+326.....	0.005	0.1	5 $< u(e) < 85$
1641+399.....	0.01	0.2	2 $< u(e) < 35$
1921-293.....	0.02	0.2	1.2 $< u(e) < 20$
2200+420.....	0.1	1.6	9 $< u(e) < 120$
2223-052.....	0.001	0.02	1 $< u(e) < 20$

A similar analysis of the centimeter spectra yields approximate values for r and B for the quiescent regions of blazars. We obtain $r \sim 10^{16}$ m and $B \sim 10^{-2}$ G.

For a source at a redshift of 0.5, and assuming $H_0 = 100 \text{ km s}^{-1} \text{ Mpc}^{-1}$, the values derived above for the quiescent and flaring regions give angular diameters of $\sim 10^{-3}$ and 10^{-4} ", respectively, indicating that the flaring regions are probably not at present resolvable using VLBI observations but that the quiescent regions may be resolvable, especially using millimeter VLBI observations (resolution $\sim 10^{-4}$ ").

VI. CONCLUSIONS

1. We have obtained a large amount of data on a sample of 11 blazars through monitoring programs performed at centimeter to optical wavelengths. The continuum spectral shape of these sources indicates the presence of at least two synchrotron components, one of which becomes self-absorbed at less than 3 mm, one at ~ 2 – 5 cm.

2. OVV quasars generally show evidence for optical/ultraviolet excesses which can be identified with the presence of one or more additional spectral components, possibly thermal in origin, such as have been proposed to account for similar excesses seen in the spectra of low-polarization quasars and Seyfert 1 galaxies.

3. The range of spectral index observed at far/mid-infrared, near-infrared, optical, and ultraviolet wavelengths can be explained in terms of emission from a power-law energy distribution of electrons $N(E) = KE^{-2.5}$, which experience recurrent bursts of injection/reacceleration and subsequently lose energy radiatively.

L. M. J. B. and D. H. H. acknowledge the receipt of SERC Research Studentships, and W. K. G. acknowledges the receipt of an SERC Postdoctoral Research Assistantship. A. G. S., D. W. S., and J. R. W. are grateful for the support of the National Science Foundation, under grant AST-88516269. We also gratefully acknowledge UKIRT Service observations for much of the infrared data. We thank the referee, Lawrence Rudnick, for helpful suggestions to the paper.

REFERENCES

- Aller, H. D., Aller, M. F., Latimer, G. E., and Hodge, P. E. 1985, *Ap. J. Suppl.*, **59**, 513.
 Barbieri, C., Cristiani, S., Omizzolo, S., and Romano, G. 1985, *Astr. Ap.*, **142**, 316.
 Bregman, J. N., *et al.* 1984, *Ap. J.*, **276**, 454.
 ———, 1986, *Ap. J.*, **301**, 708.
 Brindle, C., *et al.* 1986, *M.N.R.A.S.*, **221**, 739.
 Brown, L. M. J. 1988, Ph.D. thesis, CNAAP, Lancashire Polytechnic, in preparation.
 Brown, L. M. J., *et al.* 1986, *M.N.R.A.S.*, **219**, 671.
 ———, 1989, *Ap. J.*, **340**, 150 (Paper IV).
 Burbidge, G. R., Jones, T. W., and O'Dell, S. L. 1974, *Ap. J.*, **193**, 43.
 Burstein, D., and Heiles, C. 1982, *A.J.*, **87**, 1165.
 Clegg, P. E., *et al.* 1983, *A.J.*, **273**, 58.
 Doroshenko, V. T., *et al.* 1986, *Astr. Ap.*, **163**, 321.
 Edelson, R. A., and Malkan, M. A. 1986, *Ap. J.*, **308**, 59.
 Gear, W. K., *et al.* 1985, *Ap. J.*, **291**, 511 (Paper I).
 ———, 1986, *Ap. J.*, **304**, 295 (Paper II).
 Ghisellini, G., Marashi, L., Tanzi, E. G., and Treves, A. 1986, *Ap. J.*, **310**, 317.
 Glassgold, A. E., *et al.* 1983, *Ap. J.*, **274**, 101.
 Hanson, C. G., and Coe, M. J. 1985, *M.N.R.A.S.*, **217**, 831.
 Holmes, P. A., Brand, P. W. J. L., Impey, C. D., and Williams, P. M. 1984, *M.N.R.A.S.*, **210**, 961.
 Jones, T. W., *et al.* 1985, *Ap. J.*, **290**, 627.
 Kardashev, N. S. 1962, *Soviet Astr.—AJ*, **6**, 317.
 Landau, R., *et al.* 1986, *Ap. J.*, **308**, 78.
 Lawrence, A., Watson, M. G., Pounds, K. A., and Elvis, M. 1987, *Nature*, **325**, 694.
 Madau, P., Ghisellini, G., and Persic, M. 1987, *M.N.R.A.S.*, **224**, 257.
 Malkan, M. A., and Moore, R. L. 1986, *Ap. J.*, **300**, 216.
 Malkan, M. A., and Sargent, W. L. W. 1982, *Ap. J.*, **254**, 22.
 Marashi, L., Ghisellini, G., Tanzi, E. G., and Treves, A. 1986, *Ap. J.*, **310**, 325.
 Marscher, A. P., and Gear, W. K. 1985, *Ap. J.*, **298**, 114.
 McHardy, I. M., and Czerny, B. 1987, *Nature*, **325**, 696.
 Moles, M., Garcia-Pelayo, J. M., Masegosa, J., and Aparicio, A. 1985, *Ap. J. Suppl.*, **58**, 255.
 Mufson, S. L., *et al.* 1987, *Ap. J.*, **313**, 164.
 O'Dell, S. L., Scott, H. A., and Stein, W. A. 1987, *Ap. J.*, **313**, 164.
 Peterson, F. W., and Dent, W. A. 1973, *Ap. J.*, **186**, 421.
 Pollock, A. M. T., Brand, P. W. J. L., Bregman, J. L., and Robson, E. I. 1985, *Space Sci. Rev.*, **40**, 607.
 Robson, E. I., *et al.* 1983, *Nature*, **305**, 194.
 Salonen, E., *et al.* 1988, *Astr. Ap.*, in press.
 Sandage, A., Westphal, J. A., and Strittmatter, P. A. 1966, *Ap. J.*, **146**, 322.
 Seaton, M. J. 1979, *M.N.R.A.S.*, **187**, 73p.
 Simon, R. S., Johnston, K. J., and Spencer, J. H. 1985, *Ap. J.*, **290**, 66.
 Unwin, S. C., *et al.* 1983, *Ap. J.*, **271**, 536.
 Wardle, J. F. C. 1978, *Nature*, **269**, 563.
 Worrall, D. M., *et al.* 1982, *Ap. J.*, **261**, 403.
 Young, E. T., *et al.* 1985, IPAC preprint, No. PRE-008 N.

L. M. J. BROWN, W. K. GEAR, D. H. HUGHES, and E. I. ROBSON: School of Physics and Astronomy, Lancashire Polytechnic, Preston PR1 2TQ, England, UK

B. J. GELDZAHLER: Applied Research Corporation, Landover, MD 20785

M. J. GRIFFIN: Department of Physics, Queen Mary College, Mile End Road, London E1 4NS, England, UK

E. SALONEN and H. TERASRANTA: Radio Laboratory, Helsinki University of Technology, Otakaari SA, 02150 Espoo, Finland

P. R. SCHWARTZ: E. O. Hubert Center for Space Research, US Naval Research Laboratory, Code 4138, Washington, DC 20375

D. W. SHEPHERD, A. G. SMITH, and J. R. WEBB: Rosemary Hill Observatory, University of Florida, Gainesville, FL 32611

M. G. SMITH: United Kingdom Infrared Telescope, Hilo, HI 96720

E. VALTAOJA: Turku University Observatory, University of Turku, Itainen Pitkakatu 1, 20520 Turku, Finland